Centre for Geo-Information

Thesis Report GIRS-2009-19

MONITORING MININING REHABILITATION DEVELOPMENT ACCORDING TO METHODS DERIVED FROM IMAGING SPECTROSCOPY

Case study of Sotiel-Migollas, Southern Spain

Lily Paniagua Alfaro

02/07/2009

WAGENINGEN UNIVERSITY
WAGENINGEN UR

DLR

Monitoring minining rehabilitation development according to methods derived from imaging spectroscopy

Case study of Sotiel-Migollas, Southern Spain

Lily Paniagua Alfaro

800314641100

Supervisors:

Dr. Lammert Koistra, Wageningen University
Dr. Martin Bachmann, German Aerospace Agency (DLR).
Andreas Mueller, German Aerospace Agency (DLR).
Christian Fisher, German Aerospace Agency (DLR)

A thesis submitted in partial fulfilment of the degree of Master of Science
at Wageningen University and Research Centre,
The Netherlands.

July 2nd, 2009
Wageningen, The Netherlands

Thesis code number: GRS-80436
Thesis Report: GIRS-2009-19
Wageningen University and Research Centre
Laboratory of Geo-Information Science and Remote Sensing

Abstract

The Sotiel Migollas mine complex is part of the Iberian Pyrite Belt region in Southern Spain. This area has been used for mining since Roman times. More recently, the Sotiel mine was exploited for silver and copper extraction in 1984. It was abandoned in 2002 and some rehabilitation activities have taken place since 2006. Several flight campaigns organized by DLR have flown the mine site and HyMap images were taken during the period it was active, abandoned and rehabilitated. This thesis project aims to evaluate the opportunities to monitor rehabilitation development between 2004 and 2008 in the Sotiel Migollas mine according to methods derived from imaging spectroscopy such as mineral characterization and boundaries delimitation by describing the main changes through this period of time and analyzing advantages and limitations from each method. Two main areas within the study region were analyzed and described: the mining area where rehabilitation measures had started and tailing area that is in an abandon state. For the mining area, completed rehabilitation measurements have been monitored and reflected almost no coverage of tailings related minerals. Areas where there is still presence of tailing related minerals in 2008, are in a further stage of oxidation than in 2004. Abandoned tailing areas do not preset drastic changes but transition of oxidation states are located where water runs off into the Rio Odiel. A new method is proposed by defining tailing boundaries based on image scene statistics of each year and not on static percentages. Imaging spectroscopy is a useful tool for characterizing mining environments. The results from this study offer validation of rehabilitation efforts, and guidance of areas that still need attention. Results could be useful in describing what may be occurring in other mines from the region, that have similar characteristics as those studied in these project. Information retrieved presents a valuable contribution to mine managers who usually do not have access to an spatial assessment of the mine environment. The integration of mine managers with scientist could benefit the development and application of methods to monitor mining rehabilitation.

Acknowledgements

I would like to thank my supervisor at Wageningen, Lammert Kooistra, for his availability and guidance through this process. To all the Spectroscopy Group at DLR it was a delightful experience working with all of you. Special thanks to Wieke Heldens and Martin Bachmann for their daily support and patience. Thanks to Andreas Mueller for this life enriching opportunity and his generous support. Lucia Yanez for her advices and friendship and all the lovely people I met in Wageningen.

To the endless source of inspiration, love and respect: my family. Thanks to my brothers for being so strong and supportive. My mom the bravest and strongest person in the whole world and my dad for his unconditional support, caring and patience during this difficult time. Despite the distance, I hope you all also felt my love and company.

Last but not least, I would like to thank my love and dearest friend Marco Nocita for a visit that changed my life in the most beautiful way I could ever have imagined.

Table of contents

Page

Abstract……V
Acknowledgements……VI
Table of contents……VII
List of figures……IX
List of tables……XII
Chapter:
1. Introduction……1
1.1 Context and background ……1
1.2 Problem definition……2
1.3 Research objective …… 4
1.4 Research questions……4
1.5 Report overview……4

2. Literature review……5
2.1 Acid Mine Drainage……5
2.2 Reflectance spectroscopy……7
2.2.1 Spectral properties of materials related to the study……8
2.2.1.1 Vegetation……8
2.2.1.2 Soil……10
2.2.1.3 Oxidized tailings……10
2.3 Monitoring actual state of mines using imaging spectroscopy……11
2.3.1 Mineral characterization……11
2.3.2 Predicting pH level……12
2.3.3 Surface coverage boundaries delimitation……13

3. Materials and methods……14
3.1 Case study……14
3.1.1 Mine description……14
3.1.2 Geological settings……14
3.1.3 History of mine operations……14
3.1.4 Rehabilitation process……15
3.1.5 Case study description……16
3.2 Data acquisition and data processing……17
3.2.1 Introduction……17

3.2.2 Field campaign……..…18
3.2.2.1 Calibration sites……..18
3.2.2.2 Soil samples……...19
3.2.3 Laboratory spectral measurements……..20
3.2.4 Spectral measurements processing…….....20
3.2.5 X-Ray diffraction (XRD)…….....20
3.2.6 Airborne imagery…….....20
3.2.7 Image pre-processing…….....….21
3.2.8 Validation of data sets…….....22
3.2.9 Mosaiking and definition of study area……23
3.3 Application of methods……..…24
3.3.1 Mineral mapping……..….24
3.3.2 Boundary delimitation…….28
3.3.3 Validation……..…..29

4. Results……..…31
4.1 Chemical and spectral analyses……..…31
4.2 Processing of data sets……..…32
4.3 Mineral mapping……..…34
4.3.1 Tailing related endmembers…….....34
4.3.2 Mineral mapping method……..…..35
4.3.3 Endmember identification……..36
4.3.4 Mineral maps…….....38
4.4 Boundaries delimitation…….....…45.
4.5 Validation of mineral maps and boundaries delimitation……..48

5. Discussion……..52

6. Conclusions and recommendations……56

References…….....58

Appendices……..…….....63

List of figures

Figure 1: Surveyed exploitations in the province of Huelva in Andalucia, Spain 3

Figure 2.1: Formation of secondary sulphate minerals from oxidation of pyrite in mine wastes environment. Model adapted by Zabcic (2008)……...6

Figure 2.2: An idealized sequence of acidity level and metal leachability according to Swayze et al. (2000)……..7

Figure 2.3: Reflectance spectra of green and dry vegetation and Fe-bearing secondary minerals (Clark et al., 1993). c) Spectra of mineral soils representing different soil characteristics, organic dominated (A), minimally altered (B), iron affected (C), organic affected (D) and iron dominated (E) (Stoner and Baumgardner 1981).....9

Figure 2.4. Boundary delimitation method developed by Richter (2004) in Komkotia mine, Canada. Boundary thresholds were mapped according to isolines in transition areas of vegetation and tailings (a), this thresholds were used to classify the image into land cover classes.(b).....13

Figure 3.1: Location of the Iberian Pyrite Belt and study area…….....14

Figure 3.2: Diagram of Mine activities and Hymap image coverage……16

Figure 3.3: Workflow chart of the process involved for this study…….....17

Figure 3.4. Red dotted line indicates the areas were soil samples were collected in the eastern side and northern edge of the ashes dam in the Sotiel-Migollas mine during the field campaign of 2008.....19

Figure 3.5: Description of study area over mosaic of 2008 Hymap images…….....24

Figure 3.6: Areas of interest for mineral characterization…….25

Figure 3.7: Examples of endmembers extracted from subsets and classified as green, dry vegetation and minerals…….26

Figure 3.8: Iterative process of defining spectral libraries based on results of RMSE of MESMA approach. Spectra representing bright areas with high RMSE values were

included in the library substituting spectra that had a low frequency in the characterization of minerals in the area……..27

Figure 4.1: Reference spectra for a mineral found in field and laboratory spectra of sample 1……31

Figure 4.2: Example of mixture of elements found in samples 14, 15 and 16……32

Figure 4.3: Spectra obtained from calibration target from field measurements vs. processed Hymap image 2008……..33

Figure 4.4: Multiplicative factors of an additional empirical line correction. Values calculated as the ratio between image and field spectra.....33

Figure 4.5: Calibration target spectra from two different flight lines of 2008……...34

Figure 4.6 Spectra of mining parking lot for 2004 and 2008……..34

Figure 4.7: Illustration of endmembers used to characterize tailing area in 2008. Comparison of changes in frequency when endmembers are used to map only the area inside the tailing or its surroundings.....35

Figure 4.8: Mapping results of tailing area in 2008 using SAM and μMESMA. Similar spectral patterns are recognized but SAM seems to show less scattered results……36

Figure 4.9: Endmembers spectra extracted from tailings and mining areas, from 2004 and 2008, labeled according to predominant minerals……..…37

Figure 4.10: Color display for minerals labeling in mineral maps from tailings and mining areas from 2004 and 2008……..…37

Figure 4.11: Mineral maps of tailing areas from 2004 and 2008……..…..39

Figure 4.12. Mineral maps of 2004 and 2008 of mining area……..….40

Figure 4.13: Mineral maps of 2004 and 2008 of mining area. .Enlargement of flotation dam……41

Figure 4.14 Mineral maps of 2004 and 2008 of mining area. .Enlargement of surrounding area of the machinery house……42

Figure 4.15. Mineral maps of 2004 and 2008 of mining area. .Enlargement of ashes dam……43

Figure 4.16 False color composite of Kam Kotia mine in Canada, Richter (2008) and respective abundances of green, dry vegetation and soil and minerals in Sotiel Migollas mine in Spain. Regions in blue color have no cover of its respective material whereas region with red color indicate full surface cover…….46

Figure 4.17. Tailings boundary delimitation (red area) in study area for 2004 and 2008. Enlargement of mining area…….47

Figure 4.18. Tailings boundary delimitation (red area) in tailing area for 2004 and 2008……48

Figure 4.19.. Comparison of results from this study and Zabcic (2008) for the tailing area in 2004. Similar distributional patterns are recognized in both maps and results are classified using the same endmembers labeling……..49

Figure 4.20. XRD mineral composition for field samples collected in 2008. White dotted line (not scaled) indicates the sites were sample 1-5 and 12-16 were collected in the ashes dam. Minerals found in XRD results and marked in bold are also found when labeling endmembers spectra extracted from the image of 2008……50

Figure 4.21 . Cross verification of boundaries delimitation results and mineral mapping for 2008. Area defined as tailing by the boundary delimitation method did not correspond to the areas characterized as tailing related minerals obtained from the mineral maps….51

List of tables

Page

Table 1: Major accidents related to tailings dam failure during the last 10 years (WISE, 2008)…….....2

Table 2: Absorption features of Fe-bearing secondary minerals……..…10

Table 3.1. Coverage and spectral resolution of ASD FieldSpec Pro spectrometer (Analytical Spectral Devices, 2000)…… … 18

Table 3.2. Summarized information of Calibration targets in Calanas, 2008…… ….19

Table 3.3 Hymap technical specifications (Cocks et al., 1998)……..…21

Table 4. Confussion matrix comparing results of mineral characterization using SAM and MESMA method for tailing area in 2008.....36

Chapter 1. Introduction

1.1 Context and Background

Mining activities and environmental impacts

Mining activities consists of extracting minerals with sufficient economical value from the earth's crust. Minerals of interest, commonly referred as ore, vary from time to time and from mine to mine. Many techniques are used to extract the ore from the host rock or matrix. Mining cause important environmental impacts, since processes involved relies on the usage of hazardous chemicals and imply the modifications of landscapes and groundwater systems. Major wastes produced by these processes are mine water and rock waste. Most of these wastes are recycled back into the mineral processing because of its high content of metals; others are retained and dispersed in the mine site (EPA, 2000).

Mine water refers to all the water entering the mine surface or underground area. There are different methods to stop water from entering the mine and the retained water is used for different purposes. When a mine is abandoned or inactive, water follows its normal path filling up the underground mines and surface pits. Depending on the nature of wastes, processes involved and local geochemical conditions, this water may contain high concentration of heavy metals, dissolved solids, elevated temperatures and altered pH (Salomons, 1995). Being exposed to oxygen, the present pyrites and sulphide minerals transform the water into acidic water dissolving metals contained in the mine. The runoff of this water into down-gradient ground and surface water resources is known as Acid Mine Drainage (AMD).

Under normal conditions, acid drainage is a natural weathering process. Normally it occurs very slowly and presents no significant threats to aquatic ecosystems. During mining extraction large volumes of waste rocks containing sulphide minerals are oxidized at a higher rate since more surface area is exposed to air and water (Ferrier, 1999). AMD is one of the largest problems derived from hardrock metal mining; the severity of the impacts is reflected in the contamination of surface and groundwater sources for drinking water and aquatic habitats (EPA, 2000). Mining activities represent environmental and socio-economic risks to its surrounding areas no matter if the mine is active or abandoned. Mine wastes are often stored in large dams or depositions that may have serious impacts in health of humans and equilibrium of natural ecosystems.
There have been accidents in the past related to the collapse of these dams, toxic dust and heavy metal concentration in organisms. Areas around abandoned mines are threatened

with acid or alkaline drainage that affects drinking water sources, land productivity and aquatic ecosystems (USDA, 1993).

1.2. Problem Definition

According to the United Nations Environment Programme (UNEP, 2000), in the last 30 years, 76 % of accidents related to mines are caused by tailings dam mishaps. Table 1 presents a summary of some important accidents related to dam failure in the last 10 years.

Throughout the European countries mines were closed and left abandoned without proper measurements to prevent pollution. According to Cale and Cambridge (2000) in the past 25 years many of the tailing dams that had failed occurred in under-regulated environments. Accidents as the mine dam failure in Aznalcollar in Spain 1998, were catalysts for the creation of the Mine Directive from the European Commission, as an effort to apply legislations and regulations to mining activities and rehabilitation measurements to all its state members.

Table 1. Major accidents related to tailings dam failure during the last 10 years (WISE, 2008)

Year	Country	Damage
2008	United States	4.1 million m3 of ashy slurry covered 1.6 km2 damaging homes
2008	China	Mudslide buried a market, homes and buildings. 254 people died, 35 injured
2006	China	Landslide buried mine town. 17 residents disappeared, 130 injured.
2005	United States	17 million gallons of acid liquid into marshlands
2004	Canada	tailings spilled into 5,500 ha Pinchi Lake
2003	Chile	tailings flowed 20 km downstream rio La Ligua
2001	Brazil	Mudslide of 6 km. Mine workers killed and disappeared
2000	United States	950,000 m3 coal waste release into streams
2000	Sweden	4 million m3 of liquid with residual slurry into the environment
2000	Romania	22,000 ton. released into a tributary of Tisza River
1999	Philippines	700, 000 ton. of cyanide tailings buried 17 homes and riceland.
1998	Spain	5 million m3 of toxic water into protected wetlands

As a result of this initiative, inventory assessments and European research networks were established such as the MINEO project in 2000. The regional government of Andalucia province in Spain made an effort to assess the number of exploitations in the region. According to Junta de Andalucia (2008), for the years of 2004-2005, 2136 mines were assessed from which 860 are still active and only 636 in the process of rehabilitation leaving 820 known mines left abandoned only in Andalucia. The province of Huelva, where this study takes place, has 309 known existing mines, where 81 are active, 153 abandoned and 75 rehabilitated (fig 1). This survey is an effort to make an inventory of the exploitations in

the region and is still an ongoing project. Information about rehabilitated mines and how its success is monitored or measured is not available or little known.

Important efforts have been developed in creating techniques that monitor the state of mines in cost-effective, non-risky and non-invasive ways, such as information derived from imaging spectroscopy (Bedini et al., 2009; Kemper 2003; Ferrier, 1999). Characterizing mining environments in a rapid and efficient way is necessary to assess its state and orient remediation efforts. Some of these are: mineral characterization, prediction of pH level and delimitation of land cover boundaries (Swayze et al., 2000; Ong and Cudahy, 2002; Ong et al., 2003; Kemper, 2004; Zabcic et al., 2005; Zabcic, 2008; Richter, 2008). It is important to study limitations and advantages in the application of methods derived from imaging spectroscopy in time series analysis in order to evaluate its implementation for monitoring rehabilitation measurements.

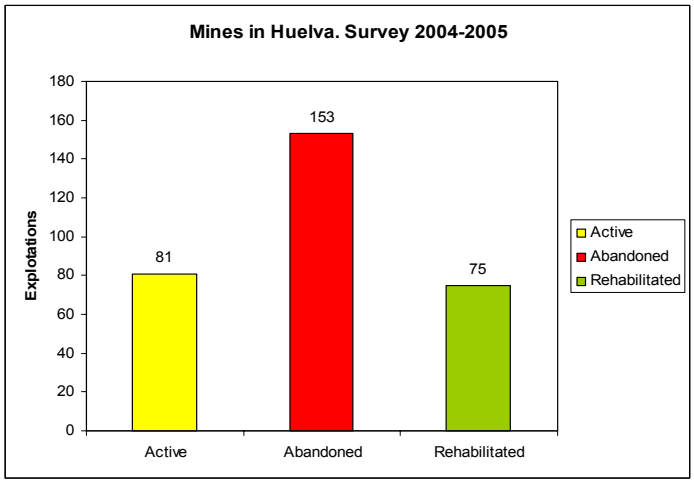

Figure 1. Surveyed exploitations in the province of Huelva in Andalucia, Spain (Junta de Andalucia, 2008).

1.3. Research objective

The objective of this thesis is to assess the opportunities to monitor rehabilitation development between 2004 and 2008 in the Sotiel Migollas mine according to methods derived from imaging spectroscopy such as mineral characterization and boundaries delimitation.

1.4 Research questions

The objective leads to the following research questions:

- According to the mineral characterization method, what are the significant changes when the mine was rehabilitated?
- According to the results of boundaries delimitation method, what are the significant changes when the mine was rehabilitated?
- What were the main limitations when applying each method?
- What were the main contributions from each method?
- Are the methods derived from Imaging Spectroscopy suitable to evaluate goals of local regulators?

1.5 Report overview

The following Chapter 2, provides the theoretical framework that explains the chemical and geological background behind acid mine drainage. It explains how the materials related to this study interact with electromagnetic energy and describes their spectral properties. Finally it introduces remote sensing techniques developed to monitor state of mines.

Chapter 3 refers to materials and methods, starts describing the study case of the Sotiel-Migollas Mine in Huelva, Spain and describes the steps involved in data acquisition, processing and application of the studied methods: mineral characterization and boundaries delimitation.

Results are described in Chapter 4 and a discussion of those results is detailed in Chapter 5. Chapter 6 is an overview of relevant conclusions and further recommendations of the study.

Chapter 2. Literature Review

2.1 Acid Mine Drainage (AMD)

AMD geochemical processes

Acidity and high concentrations of metal ions are the main factors that cause AMD to be considered as an environmental hazard (Richter, 2004). The availability of hydrogen ions is referred as acidity; the intensity of this concentration is described with the pH level. AMD are characterized by low pH values and high acidity regions, this causes an increase of the solubility of metal ions such as aluminium, copper, zinc, cadmium, among others (Kemper, 2003). Depending on the organism, each of these minerals is dangerous at different concentrations, although the conditions presented at AMD are generally known to be very toxic (EPA, 2000).

The oxidation process of sulphide minerals, as pyrite, is accelerated by its exposition to air and water due to the rock crushing and grinding process of mining (Ferrier, 1999). The formation of AMD is a product of a cyclic process of four geochemical reactions described Singer and Stumm (1970). The cycle is fed by the availability of ferric iron or pyrite.

$2\ FeS_2 + 7\ O_2 + 2\ H_2O \rightarrow\ 2\ Fe^{2+} + 4\ SO_4^{2-} + 4\ H^+$ .....(Equation 1)

$4\ Fe^{2+} + +\ O_2 + 4\ H+ \rightarrow 4\ Fe^{3+} + 2\ H_2O$ .....(Equation 2)

$4\ Fe^{3+} + 12\ H_2O\ \rightarrow 4\ Fe(OH)_3 + 12\ H^+$ .....(Equation 3)

$FeS_2 + 14\ Fe^{3+} + 8\ H_2O \rightarrow 15\ Fe^{2+} + 2\ SO_4^{2-} + 16\ H+$ .....(Equation 4)

The first equation describes oxidation of pyrite to produce ferrous iron, sulphate and acidity under the presence of air and water.

The second reaction is determined as the “rate determination” by Singer and Stumm (1970). In this step once the pyrate oxidation and acid production starts, a bacteria (i.e. *Thiobacillus ferroxidans*), under optimal conditions of low pH, accelerates the reaction rate.

During the third reaction more solid ferric hydroxide and acidity are produced due to the hydrolysis of ferric ion with water. The fourth stage is related with the oxidation of pyrite by ferric iron. The cycle continues until ferric ion or pyrite from reactions 2 and 3 are no longer available. A series of Fe-bearing secondary minerals become soluble in AMD. The

solubility of the minerals depends on various factors such as: pH, degree of oxidation, moisture content, and solution composition (Salomons, 1995). Figure 2.1 describes the reaction chain of the oxidation of pyrite and the precipitation conditions for the formation of secondary sulphate minerals.

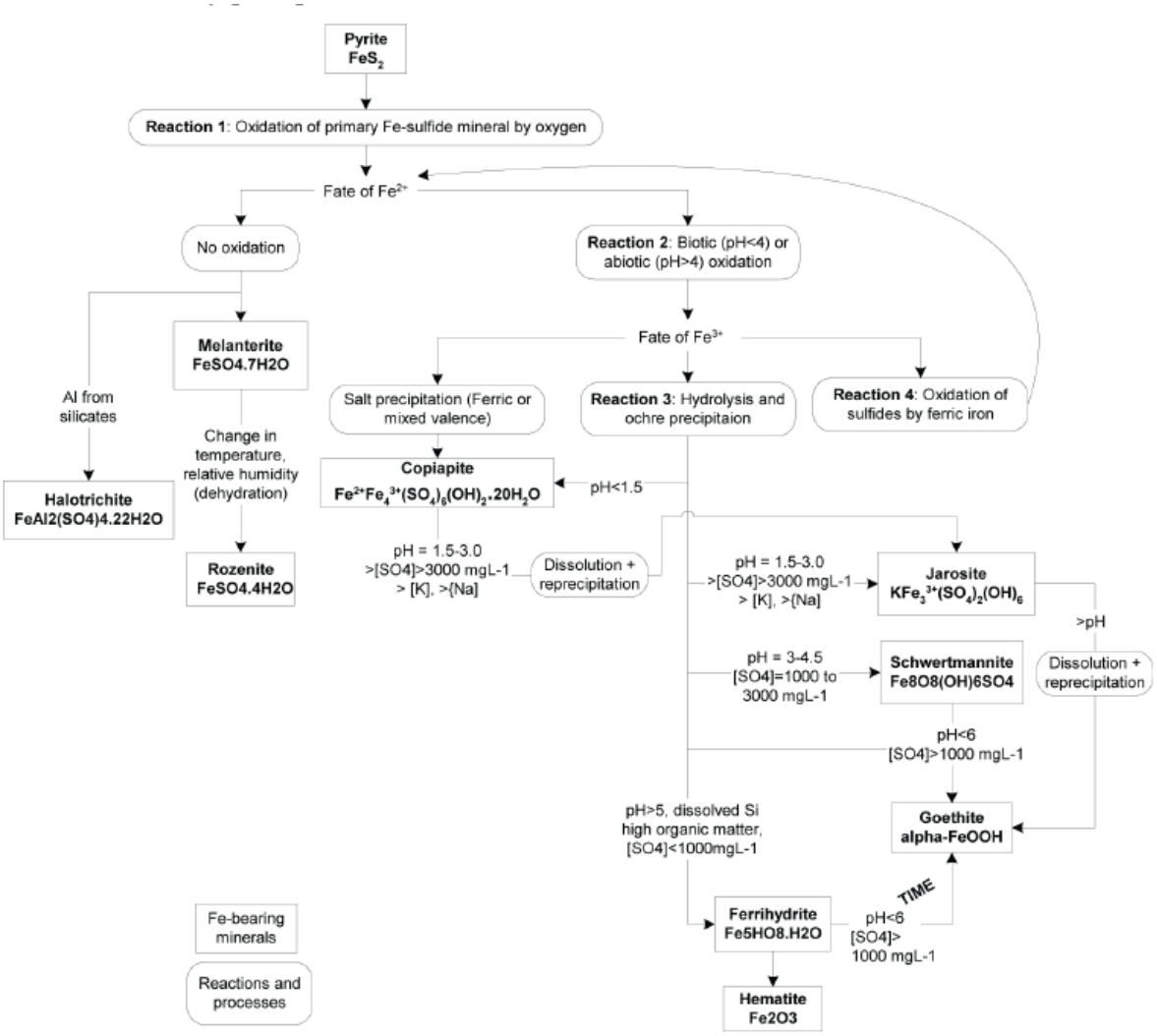

Figure 2.1 Formation of secondary sulphate minerals from oxidation of pyrite in mine wastes environment. Model adapted by Zabcic (2008).

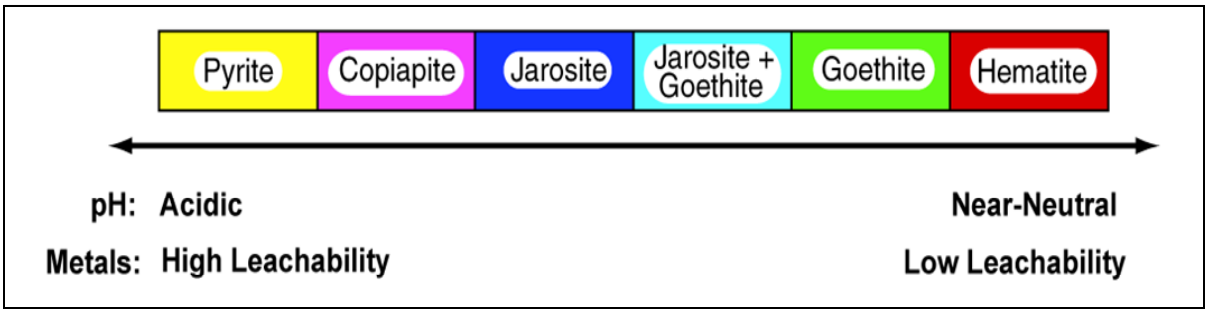

Figure 2.2 An idealized sequence of acidity level and metal leachability according to Swayze et al. (2000).

The presences of the minerals described in Fig 2.1 are indicators of the stage in which AMD is generated or neutralized. For example, copiapite precipitates at early stages of the oxidation process. Once the availability of iron to be oxidised is finished ferrihydrate or jarosite could eventually reach saturation. With exposure to dilute waters with higher pH levels jarosite could decompose to goethite. The later could dehydrate into hematite. The occurrence of these mineral can provide a guide to spatially locate potential acid generating areas (Swayze et. al 2000) (figure 2.2).

2.2 Reflectance Spectroscopy

Light as a function of wavelength interacts with matter. Spectroscopy is the study of the behaviour of the wavelengths after they had interacted with matter. Understanding the interactions of matter with electromagnetic energy is key to derive information of the surfaces being observed (Goetz, 1985).There are different mechanisms during this interaction that affects the entire or some parts of the spectrum. The region of the spectrum where a material absorbs most of the energy is known as an absorption feature.

The spectrum has been arbitrary divided into different spectral or wavelength ranges. For this study the ranges of interest are defined as in remote sensing literature being from 0.4-1 μm as the visible/infrared region (VNIR) and from 1-2.5 μm as the short wave infrared (SWIR) (Lillesand, 1994).

Absorption features observed in narrow band regions are associated to electronical and vibrational molecular processes. The electronical process occur at the VNIR range and are caused by crystal field effect, charge transfer absorptions, conduction bands and colour centres The vibrational processes take place at the SWIR region and are related to the vibration frequency of covalent bonds. The absorptions are caused by vibrations of covalent bonds such as OH, H2O (Clark, 1999; Salomons, 1994).

2.2.1 Spectral properties of materials related to the study

For the scope of this study the spectral properties of vegetation, soil and minerals are described as following.

2.2.1.1 Vegetation

Vegetation spectra can be grouped in two categories green vegetation and dry non-photosynthetic vegetation. Vegetation spectra are characterized by the absorption features caused by chlorophyll pigments a and b around 0.4-0.7 μm. Cell structure influences the absorption at 0.7-1.1 μm (Goetz, 1985). A gradient reflectance between the visible part and near infrared is known as the “red edge”, it is an important indicator for vegetation stress. Green vegetation is characterized by the absorption of pigments and also for the presence of water in the SWIR region (Lillesand, 1994).

Dry vegetation has no chlorophyll and less water absorption than green vegetation, therefore is recognized by the absorptions features caused by cellulose (1780 nm, 2100 nm, 2270-2280 nm) and lignin (1450 nm,1680 nm,2050 nm and 2150 nm) (Clark, 1999). Figure 2.3a shows the difference in spectra an important absorption features of green and dry vegetation

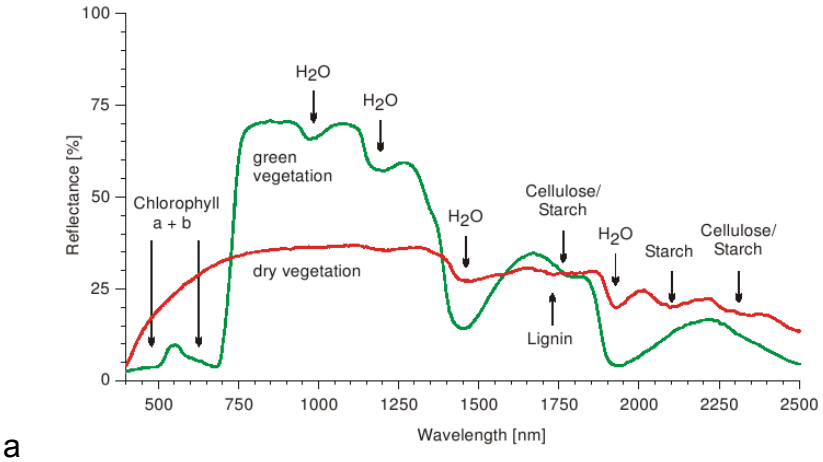

a

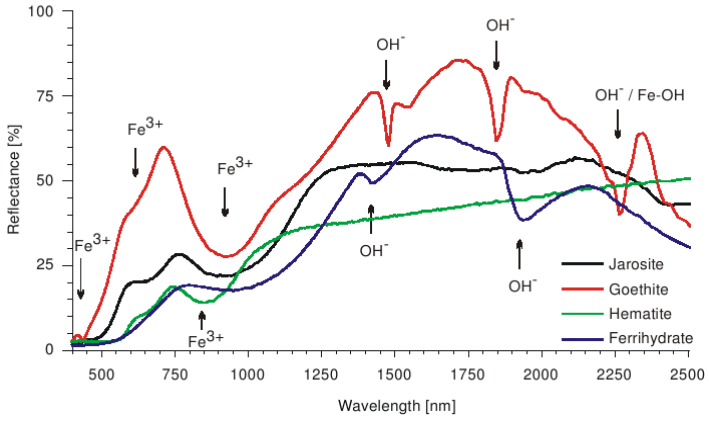

b

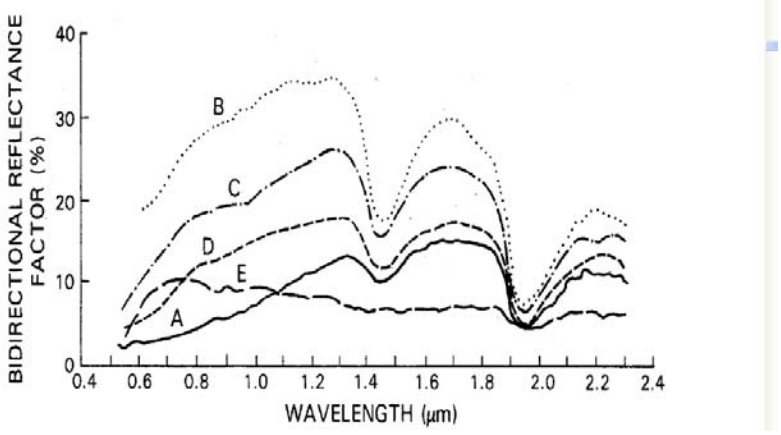

c

Figure 2.3. a),b) USGS reflectance spectra of green and dry vegetation and Fe-bearing secondary minerals, respectively (Clark et al., 1993). c) Spectra of soils representing different soil characteristics, organic dominated (A), minimally altered (B), iron affected (C), organic affected (D) and iron dominated (E) (Stoner and Baumgardner 1981).

2.2.1.2 Soil

Soil is a composition of different minerals, organic matter, iron, water and salinity. The combination and amount of each component result in a different spectral reflectance (Ben-Dor et al., 1999). Some studies have identified five basic curve shapes associated with soil characteristics based on visual interpretation (figure 2.3c).

2.2.1.3 Oxidized tailings

Mining of metallic sulphide ore deposits generates huge amounts of mining waste. This waste produces acidic water through chemical reactions of surface water with sulphur bearing minerals like pyrite. Its identification is based on spectral properties of pure minerals and mixtures of them. Mine related minerals are traceable due to the presence of secondary minerals products of the oxidation of pyrite. Pyrite itself is difficult to identify due to its low reflectance, saturated Fe absorptions and opaque coating (Swayze et al., 2000), therefore the key elements to identify are iron oxides, hydroxides sulphates and sulphides.

From the transition elements, iron is present in many minerals and relatively easy to detect. Important absorption features, due to its valence characteristics (Fe^{2+}, Fe^{3+}), occur at 550 nm, 650 nm and 900nm. There is an important contrast at SWIR reflectance at 700-1000 nm due to crystal field effects (Clark, 1999). The combination of absorption features in the VNIR and SWIR region (Table 2, Figure 2.3b) provides enough information to identify important secondary minerals derived from AMD (Salomons, 1995)

Table 2. Absorption features of Fe-bearing secondary minerals

Mineral	**NIR (0.4- 1.5 µm)**	**SWIR (1.5- 2.5 µm)**
Jarosite	0.43 (Fe2+), 0.91(Fe3+)	2.27(OH, FE-OH), 1.475, 1.8 (OH) common for sulphates
Copiapite	0.43(Fe2+)	1.475, 1.950 (OH)
Ferrihydrate (Fe(OH)3)	1.0(Fe3+)	1.45, 1.950(OH/H2O)
Goethite (FeO(OH))	0.48, 0.65, 0.92 (Fe3+) 0.55 (conduction band) trans-opaque behaviour 0.9 (Fe3+)	
Hematite (Fe2O3)	Similar to goethite 0.9 (Fe3+) narrower and at shorter wavelength than goethite	

2.3 Monitoring actual state of mines using imaging spectroscopy

Reflectance spectroscopy is used to derive significant information of materials, since it is based in electromagnetic radiation reactions there is no need for sample preparation like other laboratory analysis. Is a method that can be used for measurements in laboratory, field and airborne or space spectrometers. When used in hyperspectral airborne remote sensing it provides the potential of spatial observations of affected areas at different spatial resolutions (Kemper 2003). Therefore is an excellent tool to identify materials that exhibit distinct absorption features in the electromagnetic spectrum. Among these are iron oxides, iron hydroxides and sulphates which are the main focus for identification of mine tailings. Due to its potential in spatial recognition, imaging spectroscopy provides an accurate and efficient non invasive technique to pinpoint sources of acidity (Bedini et al., 2009; Kemper 2003; Ferrier, 1999).

According to Kemper (2003), only when measuring at a laboratory, controlled conditions can be assumed. Nowadays it is possible to account for most of limitations and challenges when measuring with field or airbone spectrometers but is important to be aware of them. When measuring in the field or from airborne system, illumination conditions by the sun can be affected by the atmosphere. It is also important to take into account that the area of measurement, determined by the pixel size and the spatial scale of the sensor, is usually not an homogenous area causing a mixture of different elements in the field of view. Another limitation is that meaningful physical and chemical properties cannot be measured directly so a combination of field and remote sensing observations have to be calibrated with those properties.

Different methods developed from remote sensing techniques are recommended for monitoring mining environments. Characterizing mining environments in a rapid and efficient way is necessary to asses its state and orient remediation efforts. Some of these are: mineral characterization, prediction of pH level and delimitation of land cover boundaries. Each of them provides different types of information that could be complementary to each other if applied to same data sets of active or inactive mines. A description of methods to characterize mine environment is detailed below.

2.3.1 Mineral characterization

This method provides the recognition of secondary minerals present on the mine tailings (Kemper, 2003; Kemper et al. 2005; Swayze 2000; Zabcic 2008). An important factor of mineral characterization it that it recognized the hydrated state of the minerals, this

information serves as an indicator of pH levels, metals and sulphates present at the time of the image. It also provides the baseline to predict which chemical reactions would occur when local conditions vary such as climate and weather.

Dennison et al (2004) describe different spectral matching algorithms that can be used for mineral characterization based on the identification of unknown spectra and its similarity with one or more known spectra. Two popular algorithms are the multiple endmember spectral mixture analysis (MESMA) and the spectral angle mapper (SAM). MESMA , functions as a linear mixing model that displays an error metric by a root mean square error. It is based on spectral mixtue analysis (SMA) which uses a “shade” edmember to account for variations in spectral albedo. SAM compares two spectra using a spectral angle error metric. It resolves spectral similarity by calculating a spectral angle between two spectral vectors that have a common origin. This angle functions a s the error metric for this method.

2.3.2 Predicting pH level

Knowing the pH conditions of the mine is an orientation to the different types of oxidation reactions occurring at the mine (Ong et al., 2003; Ong and Cudahy, 2002; Swayze et al., 2000; Zabcic et al., 2005; Zabcic, 2008). This information is valuable to precisely point out which areas required neutralization methods and could also be useful in calculating quantities or concentrations of neutralizing products to be applied. Information regarding pH could also be derived from mineral maps; this information derives from known ranges where the secondary minerals could occur. Some minerals precipitate on a wide range of pH values, therefore results from predicting pH levels are more precise than results derived from mineral characterization (Zabcic, 2008).

Traditional measurements of chemical properties, as pH level, can determine pollution level at point locations but they do not offer any information about their spatial structure. This can only be achieved at certain extent with spatial interpolation algorithms. However this method is highly dependent of the number and distribution of the sampling points. The most common approach for calculating pH is by establishing a relationship between pH measurements and hyperspectral data. The development of predictive models is based on the multivariate calibration technique of partial least square (PLS) analysis (Zabcic 2008; Ong et al. 2003). To build a pH predictive model, PLS calibration focuses on developing a relationship between the reflectance spectrum and the known pH of mineral soil samples. PLS descomposes the input variables into smaller set of orthogonal variables called factors, where the covariace between two is maximized. The first factors contain the most relevant information present in the reflectance measurements, the last factors represent random noise to be discarded from the model (Haaland 1988).

2.3.3 Surface coverage boundaries delimitation

With this method tailing areas, transition areas and surrounding land covers are delimitated (Richter, 2004; Richter et al., 2008; Levesque and Staenz, 2004). A method to delineate tailings area can be used to monitor the changes over the years, it also allows the estimation of the enclosed tailings area and serve as baseline for comparison with subsequent site investigations in future years.

This method developed by Richter (2008) consist on performing a spectral mixture analysis to unmix each pixel into its endmembers. Zones were defined as vegetation zone, transition zone, residues and tailing zone. Thresholds to delimit the boundaries were defined according to isolines in narrow transition areas, The mining area was classified according to the delimited zones and areas were calculated for future monitoring assessments (Figure 2.4)

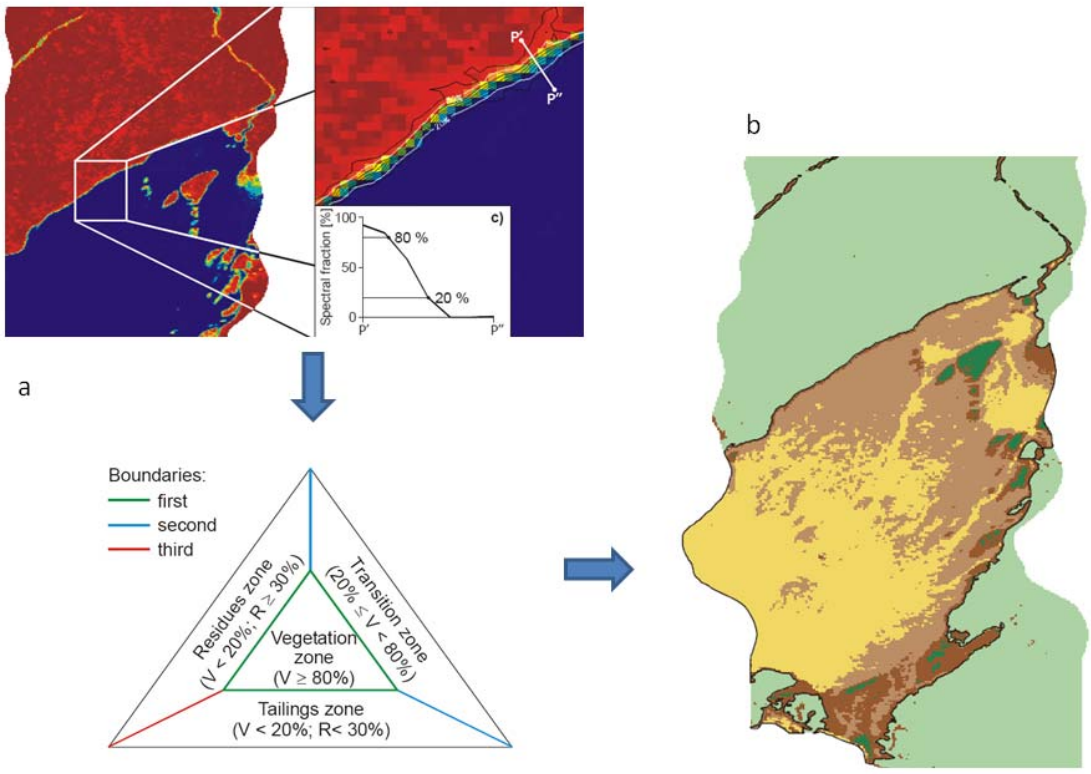

Figure 2.4. Boundary delimitation method developed by Richter (2004) in Komkotia mine, Canada. Boundary thresholds were mapped according to isolines in transition areas of vegetation and tailings (a), this thresholds were used to classify the image into land cover classes.(b).

.

Chapter 3. Materials and Methods

3.1 Case Study

3.1.1 Mine description

This study takes place in the Sotiel-Migollas mine complex in South Spain. This mine was used mainly for the extraction of lead, zinc and copper. It is part of the Iberian Pyrite Belt (Espinoza et al., 2000). The mine consisted of two tailing dams, three waste rock deposits and a processing plant. It is situated near the locality of Calanas, Andalucia inside the watershed of Rio Odiel. Its climate is Mediterranian, characterized by long dry summers and short winters (Zabcic, 2008).

3.1.2 Geological settings

As part of the Iberian pyrite Belt, the area is located within the volcanic siliceous complex of the Upper Devonian / Lower Visean. The surface is often covered by efflorescent sulphate salts due to the capillary rise of solute elements. These surface crusts are expected to contain Fe(II)-, Zn- and Mg-hydrated sulphates (Espinoza et al., 2000).

Figure 3.1 Location of the Iberian Pyrite Belt and study area.

3.1.3 History of mine operations

The history of this mine follows the same line as other mines of the region, having periods of extensive exploitation and others of abandonment. Archaeological findings

suggested an intensive activity during Roman times. According to Espinoza et al. (2000), in 1866 modern exploration methods took place and extraction activities started in 1870 but due to economical problems it was closed in 1875. The mine was reopened in 1883 and abandoned in 1939. In 1963 it was thought that the mineral reserves were exhausted but further exploration studies concluded in reopening the mine. Since then, important infrastructure were built to extract the mine reserves. By 1980 the mine belonged to the National Institute of Industry of Spain (INI) and in 1984 underground extraction of sulfuric metals took place. Navan Resoures bought the mine in 1997 and the explotation of Sotiel, Migollas and Aguas Tenidas took place until 2002 when the company abandoned the mine. Since 2005 the local government is in charge of the stewardship and restoration measurements of the mining installments.

3.1.4 Rehabilitation process

Zinc, copper and lead were the main products extracted from the mine by means of flotation process. Chemicals such as sulfuric acid and copper sulfate were added to ore-water slurry and later on roasted in order to recover sulfide minerals. The extracted materials were collected in the flotation dam and the tailings into the ashes dam. Acid waters were treated in a cleaning plant and deposited in the Rio Odiel. When the mine was abandoned, and after intensive historic activities, the area was declared to be a potential and active focus of contamination for underground, surface waters, aquifers and soils. As a consequence the landscape was modified, the ecological habitats altered, vegetation coverage destroyed and water flows changed. In December 2002 the local government assigned to the company *Empresa Gestion Medioambiental S.A*. (EGMASA) the rehabilitation of the mine through a series of works which main objectives were: the sealing of the dams, cleaning of waste rocks, and restoration of vegetation coverage. The first phase of the rehabilitation process took place from December 2002 until December 2008. The main procedures were to assure that non treated waters were deposited directly into the river and to dry and seal the flotation dam. Currently, second phase is taking place which is expected to dry and seal the ashes dam and reestablish vegetation coverage.

The expectations of the rehabilitation process consist on:

- stabilize landforms and structures;
- protect from erosive processes;
- recover and abandonment of dams;
- an eventual productive usage of recovered areas.

3.1.5 Case study description

The Sotiel Migollas mine presents a unique situation of having almost a decade covered with HyMap images. These images were taken in 1999, 2004 and 2008, corresponding to the period when the mine was active, abandoned and initially rehabilitated, respectively (figure 3.2). In 2004 extensive field campaigns, where field data was spectrally analysed and soil properties studied, took place in order to derive mineral characterization maps and predictive pH models. These robust efforts and models developed serve as a starting point in applying them to the different time periods in order to get a sound description of the processes the mine has gone through in the last 5 years.

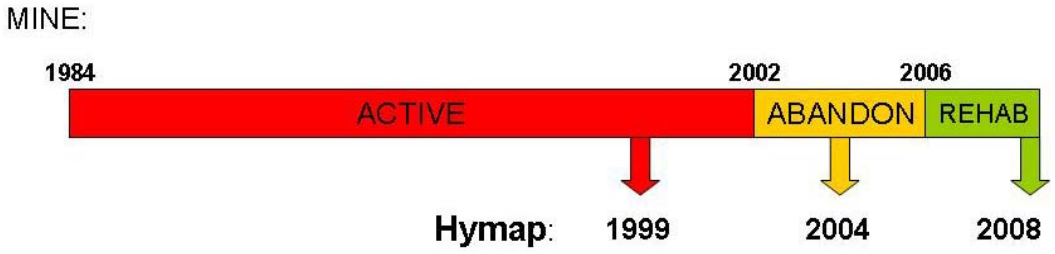

Figure 3.2. Diagram of Mine activities and Hymap image coverage.

3.2 Data acquisition and data processing

3.2.1 Introduction

This chapter describes data sets and data processing needed to reach the objectives of the study. The workflow diagram showed in figure 3.3 presents a comprehensive overview of the main steps from data acquisition to data analysis stating intermediate and output process.

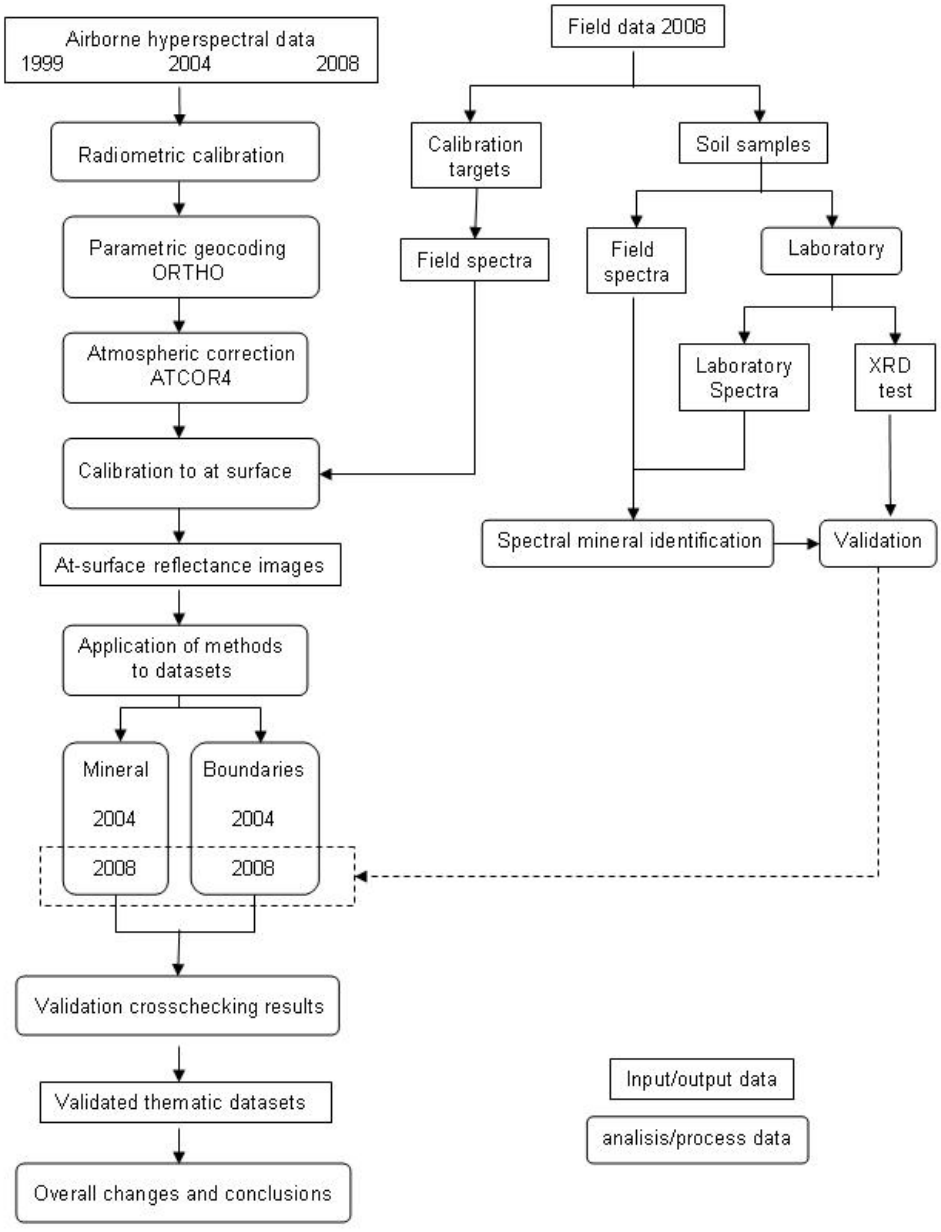

Figure 3.3. Workflow chart of the process involved for this study

3.2.2 Field campaign

The fieldwork took place as part of the over flight campaign with the HyMap sensor. Spectral measurements were taken for selected calibration targets on August 1st, 2008 as well as soil samples collected from the field on August 3rd from the same year. Spectral measurements were taken in the field using an Analytical Spectral Devices (ASD) FieldSpec Pro. This is a portable spectrometer composed of three detectors covering the wavelength range from 350 nm. to 2500 nm (table 3.1). The raw spectra collected were converted to reflectance by taking white measurements with a Spectralon reference panel.

Table 3.1. Coverage and spectral resolution of ASD FieldSpec Pro spectrometer (Analytical Spectral Devices, 2000)

Spectrometer	Bandwith	Spectral resolution
VNIR (350-1050 nm)	1.4 nm	3 (at 700 nm)
SWIR 1 (900-1850 nm)	2 nm	10-12 nm
SWIR 2 (1700-2500 nm)	2 nm	10-12 nm

3.2.2.1 Calibration Sites

Calibration sites were selected following a criteria of areas: with high reflectance, flat, homogenous, covering an area of at least 3 pixel airborne imagery size (15x15 meters or 225m²) and finally all sites should be located within the image. An average of 50 spectral measurements was taken from each calibration site. Measurements were taken using bare fiber giving a field- of- view (FOV) of 60 cm diameter at a height of 1 m. Calibration targets from past airborne survey missions were still available and used for 2008 flight campaign, these been: soccer field, basketball court, school cement yard and mine's facilities parking lot. Table 3.2 describe the location coordinates for each site and its view from aerial image and photo taken from the field.

Table 3.2. Summarized information of Calibration targets in Calanas, 2008.

Calibration Site	Description and coordinates (UTM North Zone 29)	View from field	View from 2008 Hymap Image
Mine Parking	Gravel surface- iron coating, small slope 688946 E 4168166 N		
Soccerfield	Gravel surface- fine texture, iron coating, flat surface 687374 E 4169218 N		
Basketball court	Concrete surface- red painting, flat surface 687374 E 4169218 N		
School concrete platform	Concrete surface- paved, flat surface 687358 E 4169110 N		

3.2.2.2 Soil samples

From the edges of the ashes dam, 10 areas were chosen for soil samples and spectral measurements with the Field spec were taken before they were collected (figure 3.4). The area was difficult to access, so spots that visually look different were chosen. An average of 25 spectra measurements were collected using the 8° FOV lens measuring a diameter of 15 cm from each sample. A square of approximately 7x7 cm of each sample were stored in plastic containers.

Figure 3.4. Red dotted line indicates the areas were soil samples were collected in the eastern side and northern edge of the ashes dam in the Sotiel-Migollas mine during the field campaign of 2008.

3.2.3 Laboratory spectral measurements

Laboratory spectral measurements were taken at similar conditions to that of the airborne data acquisition. Measurements were collected for the 10 soil samples collected at the field using the same ASD spectrometer as described in table 3.1. Illumination conditions were provided by two external halogen lams at zenith angle corresponding to that of the sun at the day of the 2008 image acquisition. Samples were taken with the 8° FOV lens as in the field. Sample size varied on size and different black non reflectance backgrounds were tested, finally a black paper was used covering a metallic plate. Measurements were taken at a height of 20 cm. The Fieldspec instrument was set to take 50 spectral measurements and white references were taken before measuring each sample using the same spectralon panel as in the field.

3.2.4 Spectral measurements processing

For each set of field and laboratory spectra, erroneous measurements were deleted due to oversaturation or mistakes when taking measurements. By means of multiplying the spectral bands by a gain factor, calculated by the difference between the first and second detector of the spectrometer, the “jump” correction was performed around the 1000 nm region of the spectrum. To eliminate any trace of impurities or dirt in the reference panel, it was calibrated against a clean reference panel and the resulted calibration ratio was applied to the laboratory spectra. Statistics were calculated to obtain minimum, maximum, and standard deviation of reflectance spectra of each sample.

3.2.5 X-Ray Diffraction (XRD)

To determine the main mineral components of the soil mixture of the 10 samples collected at the field, an X-Ray Diffraction test was performed to all the samples at the Institute of Mineralogy and Crystal Chemistry from University of Stuttgart.

3.2.6 Airborne imagery

For this project two datasets of imaging spectroscopy data were used. The images were taken on the following dates: May 19th 2004 and August 1st 2008. All datasets were obtained using the Hymap airborne sensor. This is a whiskbroom imaging spectrometer with 126 bands covering the wavelength range of 0.45 to 2.5 μm with contiguous spectral coverage, except in the atmospheric water vapour bands, and bandwidths between 10 and 20 nm (Cocks et al., 1998). Table 3.3 summarizes the technical specifications of the hyperspectral airborne sensor HyMap.

Table 3.3 Hymap technical specifications (Cocks et al., 1998).

Typical Operational Parameters			
Platform	Light, twin engine aircraft		
Altitudes	2000-5000 masl.		
Ground Speed	110-180 knots		
Spatial Configuration			
IFOV	2.5 mrad along track 2.0 mard across track		
FOV	61.3° (512 pixels)		
Swath	2.3 km at 5m IFOV (along track) 4.6 km at 10m IFOV (along track)		
Typical Spectral Configurations			
Module	*Spectral range (µm)*	*Bandwith across module (nm)*	*FWHM (nm)*
VIS	0.45 - 0.89	15 – 16	15
NIR	0.89 - 1.35	15 – 16	15
SWIR1	1.40 - 1.80	15 – 16	13
SWIR2	1.95 - 2.48	18 – 20	17

3.2.7 Image pre-processing

Each dataset had to undergo through the same pre-processing steps to result in an image with at-surface calibrated reflectance. These pre-processing steps are: radiometric calibration, geometric correction, atmospheric correction and verification using calibration targets. The following is a detailed description of pre-processing steps which the set of images have undergone.

Radiometric correction

HyVista provided the Hymap radiometric correction by converting the recorded Digital numbers (DN) into at sensor-radiance by using a calibrated Spectralon pad at 45° view from the sensor and a lamp that illuminates the pad at normal incidence (Cocks et al. 1998).

Parametric geocoding

The software package used for orthographic rectification is ORTHO (Müller, et al 2005). This software uses sensor specific parameters, flight parameters (sensor position, roll, pitch, etc.) and digital terrain model to derive geographically projected images without sensor movement distortions. Junta de Andalucia provided a 10 meter resolution DEM to rectify the images. Orthorectification was performed using nearest neighbour interpolation. The image was projected to 29 North UTM coordinates using as datum European mean 1950. External official paper maps, ground control points, field data and earlier geocorrected images were used to verify geographic correspondence of objects and overlapping continuity between flight lines.

Atmospheric correction

Atmospheric correction was carried out by the software package Atmospheric and Topographic Correction Model (ATCOR4), (Richter and Schläpfer, 2002). The model needs to be feed with atmospheric parameters in order to retrieve an image without any illumination effects related to topography or atmospheric influence. The parameters selected were: a standard rural aerosol type, visibility of 25 km and 0.94 μm and 1.3 μm regions were chosen to run water vapour algorithm. To correct for topographic effects the function of rugged terrain was selected and the DEM from the Junta de Andalucia applied, also a Bidirectional Reflectance Distribution Function (BRDF) was performed.

3.2.8 Validation of data sets

For the purposes of this study is important to validate that the spectra in the image is coherent with the spectra in the field, so spectra taken with a field spectrometer should be similar to the airborne sensor after the atmospheric correction was applied. As mentioned earlier both images, 2004 and 2008, were taken with the same sensor and the same processing steps took place. In order to make temporal comparison they should be validated for their spectral coherence so the changes detected are due to changes in materials during the years and not because errors in the atmospheric correction process. Finally to validate if the spectra from field measurements, laboratory and images retrieve similar information to identify materials, they were compared with the XRD field samples results.

Field spectra vs image spectra 2008

An area of interest was drawn around the calibration targets detected in the image of 2008. Within this area the average spectra was calculated and compared with the average

of field spectral measurements from the same target. Both results were compared to find if there was an agreement between both measurements. In addition to the atmospheric correction, a test with an empirical line correction was conducted to see if it improved the results.

Validation of spectra from different flight lines 2008

To validate different flight lines of the same year, calibrated targets with field measurements that occurred in the overlap of two flight lines were compared for both images. This to confirm that even though there was no ground data for 2nd or further scene/flightline, all the images corresponding to 2008 are spectrally coherent

Spectral validation between 2004 and 2008

In order to map changes between datasets is important to prove that these are due to changes in materials and not because of differences in atmospheric corrections. Therefore, average spectra of pixels from invariant calibration targets were compared between 2004 and 2008 to validate if both images are spectrally comparable.

3.2.9 Mosaiking and definition of study area

Once the images were atmospherically and topographically corrected, to eliminate distortions at the edges around the images, an edge of 5 pixels from each side was removed. Cropped images were joined in a mosaic using ENVI software. Each mosaic was composed of three flight lines from each year. After the mosaic was created, using ENVI, the following step was to define the study area. The study area covers the region from 685594- 692782N and 4170590- 4162370E UTM Zone 29 North, with an extent of approximately 4,250 hectares. The study site had to encompass the following regions: calibration targets, Calanas town, Machinery house of the mine area, waste dams and downstream area until the Odiel River. Figure 3.5 describes the study are and important regions of interest.

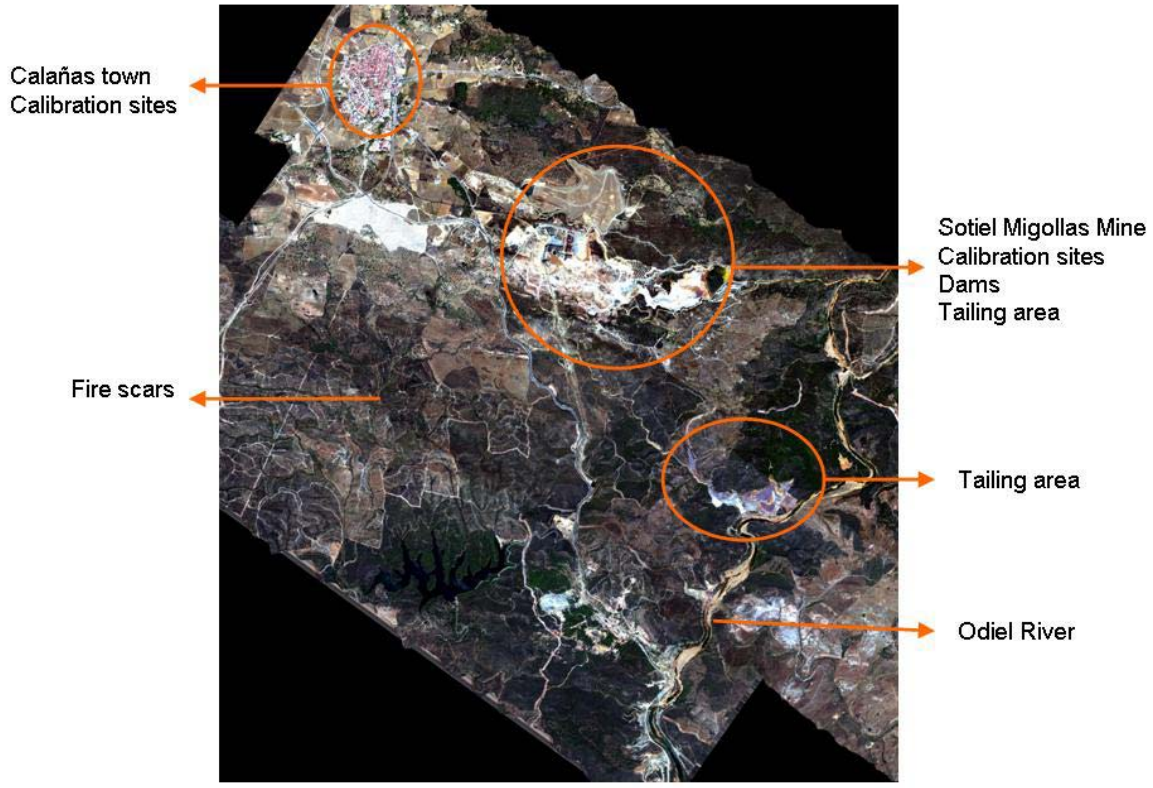

Figure 3.5 Description of study area over mosaic of 2008 Hymap images.

3.3 Application of methods

3.3.1 Mineral mapping

Each pixel of the HyMap image represents a mix spectra of elements on a 25 m2 area. For the purpose of this study, the dominant element of each pixel is identified and the spatial pattern is compared among the different data sets. Within the study area two main regions are of interest to characterize the mineral: 1. the mine area itself covering the flotation pond, waste pond and area around the machinery house, 2. tailing area next to the Odiel River. The rehabilitation process of the Calanas mine had started, so special attention is given to changes in minerals and its spatial distribution. The tailing area is expected to start its rehabilitation process in 2010 so the results could serve as a baseline for future restoration planning and monitoring. Figure 3.6 shows the two areas where the mapping characterization was applied.

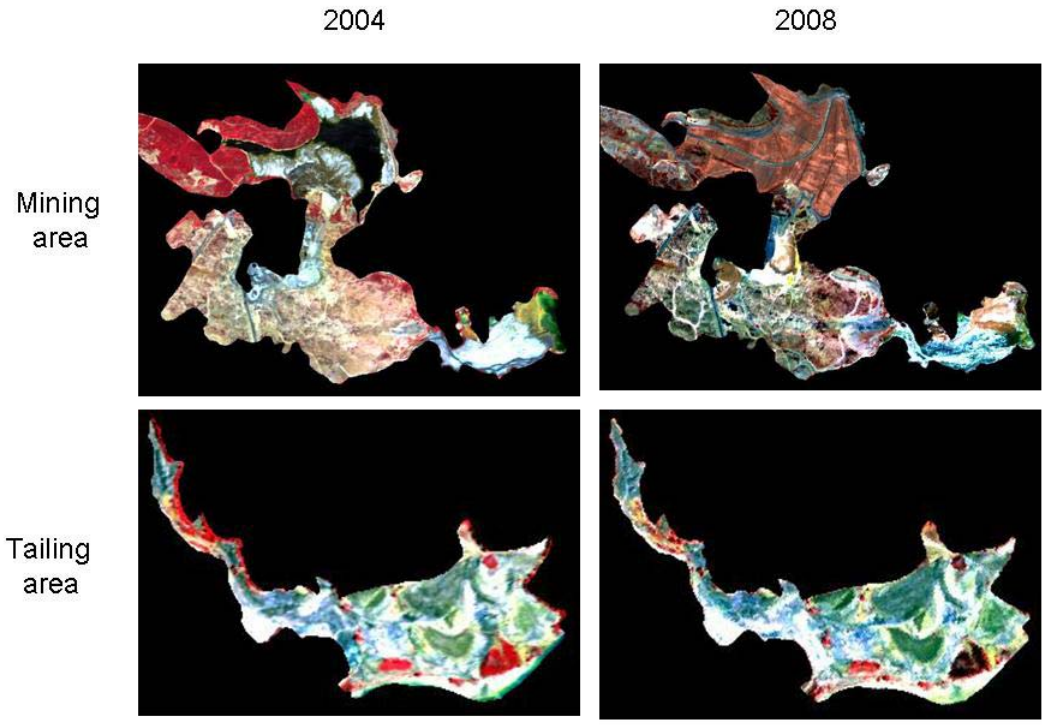

Figure 3.6 Areas of interest for mineral characterization.

For this study the main steps to characterize minerals from the two areas of interest were: endmembers extraction, selection of spectral libraries, labeling of endmembers and generation of mineral maps.

Endmember extraction

A pre-segmentation of the subsets was performed to reduce noise pixels and exclude errors. Endmembers are spectra that are chosen to represent unique surface materials in an image. Endmember extraction was performed by a sequential maximal angle convex cone (SMAAC). This method finds the brightest pixel in the image and the most different one, then it finds the pixel most different from the first two. The process is repeated until new pixels could be grouped in an already defined pixel or until a predefined number of endmembers was set. The result of SMACC does not correspond to every element in the image, although each endmember extracted is unique. The masking of the mining area and tailing area retrieves only endmembers that are of interest for the characterization of minerals.

Endmember classification

SMAAC was trained to retrieve 30 endmembers. These endmembers were further classified by visual interpretation into green vegetation, dry vegetation and minerals (fig. 3.7). Soil endmembers were mostly classified as minerals specially if an iron related and clay absorption feature was present. Endmembers classified as noise, water, infrastructure, etc were excluded. The ones classified as minerals were grouped into similar curve shapes. Average and variations of spectra from each group were selected as representatives for the mineral spectral library.

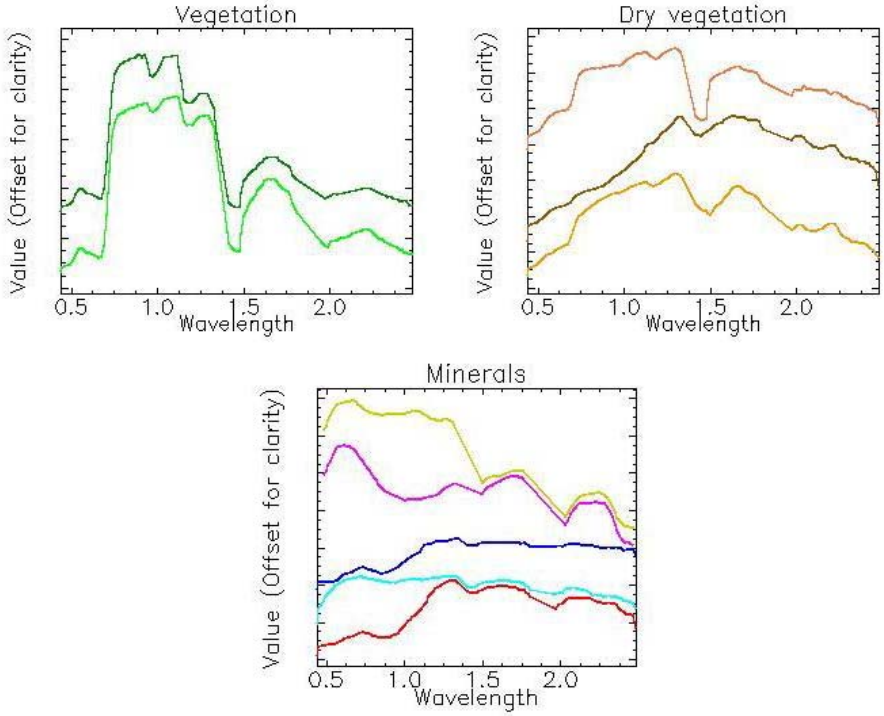

Figure 3.7. Examples of endmembers extracted from subsets and classified as green, dry vegetation and minerals.

Selection of Spectral Library

Endmembers classified as green vegetation, dry vegetation and minerals were grouped as spectral libraries to run a multiple endmember spectral mixture analysis (MESMA), a linear mixing model based on a root mean square error (RMSE). This algorithm models spectra as a linear mixture in this case of three spectral libraries (dry vegetation, green vegetation, and soil and minerals), full datasets were used and only bands in water

vapor regions excluded. Running MESMA became an iterative process, were the spectral libraries were improved by including spectra of areas that reflected high RMSE values and excluding endmembers that had a low frequency pixels assigned to that endmember. Figure 3.8 shows this iterative process, bright areas in the RMSE image corresponds to missing spectra in the libraries that feed the model, this were included to substitute endmembers that had a low frequency of pixels in the classification. This iterative process goes on until the areas of interest are well represented with the spectral library.

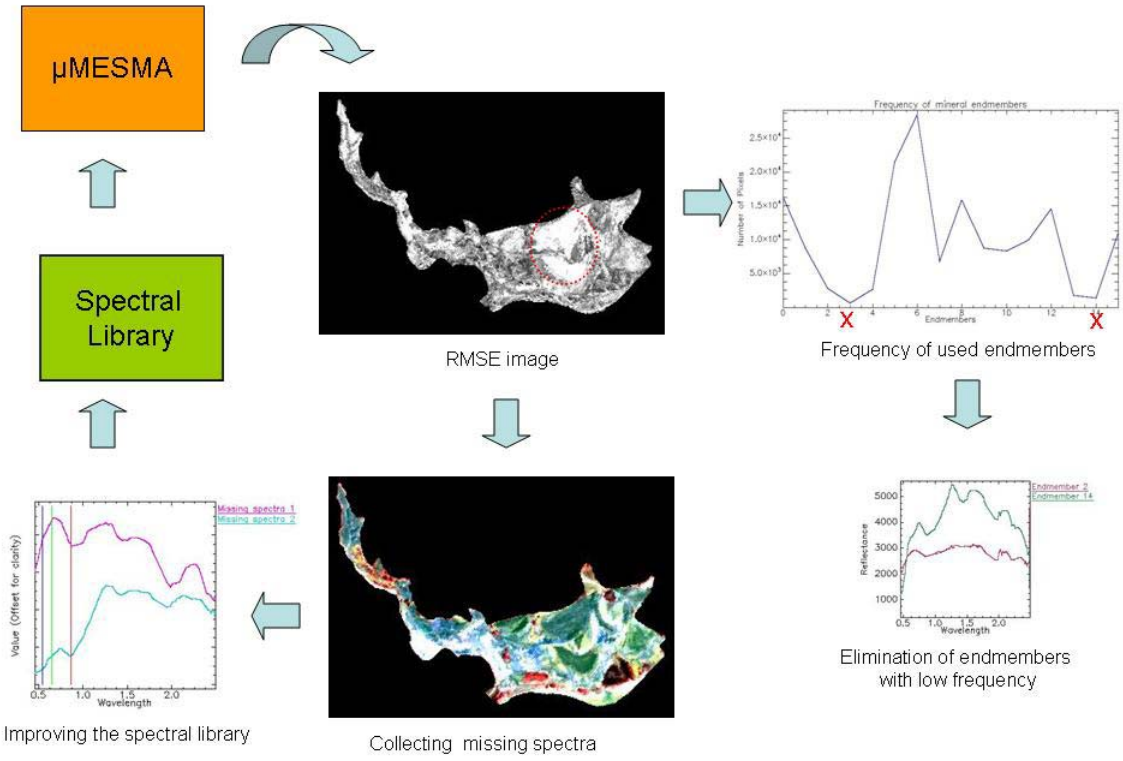

Figure 3.8. Iterative process of defining spectral libraries based on results of RMSE of MESMA approach. Spectra representing bright areas with high RMSE values were included in the library substituting spectra that had a low frequency in the characterization of minerals in the area.

Endmember mapping

Mineral characterization was performed by using Spectral Angle Mapper algorithm (SAM). This method finds spectral similarity by calculating a spectral angle between two spectral vectors that have a common origin. The spectral angle is the error metric for SAM therefore, the pixel is assigned to the endmember which has the smallest spectral angle. If the smallest angle is above a threshold of 0.1 radians, then the pixel remains unclassified.

This method is insensitive to differences in albedo, it only measures differences in spectral shape. Differences in albedo are measured by the length of each vector (Dennison et al. 2004).

Endmember labeling

Mineral labeling of endmembers classified as minerals was performed by visual interpretation, comparison between spectra library references (Grove et al, 1992; Preissler, 1999; Specmin-FE, 2003; Clark et al., 2007), XRD analysis results, results from previous studies in the area (Zabcic 2008) and expert knowledge. Absorptions features described in Appendix 1 are examples of what features and spectra curves were followed to label endmembers.

3.3.2 Boundary delimitation

This method intents to delineate the boundaries of the mine tailings and its surroundings; in order to study the interaction with the landscape and define main changes through the years. For this purpose the area of interest includes the tailing related areas from mineral mapping and it surroundings, the city of Calanas, Odiel River and cultivation areas around. The same initial procedures as for mineral mapping were performed. With SMAAC endmembers were extracted and classified as green, dry vegetation and minerals. The spectral matching algorithm used to indentify endmember in the image was MESMA. As one of the products from this algorithm are abundance maps from each spectral library used to feed the algorithm. This were used to define the thresholds to delineate boundaries.

Definition of tailing boundaries

Boundaries definition suggested by Richter (2008) could not be applied to this study site after unsuccesfull tests. Therefore a new approach in defining boundaries was performed. MESMA classifies each pixel of the image according to its abundance of green vegetation, dry vegetation and minerals. One of the outcomes of this algorithm is abundance maps for each of the spectral libraries used to feed the model. Mineral abundance map was selected to define the tailing boundaries. The main reason to select this parameter is because it's a variable that is expected to be relatively constant throughout the seasons so should not be affected by the time the images were taken. Therefore vegetation and dry vegetation were considered as a whole and pixels with tailings were

considered those were there was no presence of vegetation or dry vegetation. The threshold was defined as the sum of the media and the positive standard deviation for both time series. In both cases this threshold was defined around an abundance of minerals above 30% on each pixel. Pixels that presented these conditions were defined as tailings.

3.3.3 Validation

Endmembers classified as minerals

The frequency of selected endmembers as minerals were analyzed in the mining area and its surroundings to distinguish a different composition of materials of the mine and outside.

Mineral mapping method

The tailing area from 2008 was the test site to compare two different mapping methods and the similarity of their results. The selected spectral libraries from that area and year were used to run MESMA and Spectral Angle mapper (SAM) to analyze if there were any differences regarding which method was used.

Endmember identification

Field and laboratory spectral data corresponding to the field samples were identified using spectral reference resources. The results were compared to the mineral composition of the samples according to the XRD results. This also served as an exercise for training to use the references for further identification of endmembers extracted from the images.

Mineral characterization

The results of the mineral characterization for the image of 2004 were compared to the results obtained for the same region and year by Zabcic (2008). Both mineral characterizations were created using different methods but should be comparable in terms of spectral patterns and main composition of minerals.
Mineral mapping of 2008 was validated with samples collected in the field and later identified with XRD analysis. These should also present some spatial and material agreement with the maps of 2004.

Boundaries delimitation

Boundaries delimitation was cross verified with the ones of mineral mapping. They should be coherent in terms of areas identified as tailings. Information gathered during field visit and expert knowledge also served as validation of the maps.

Chapter 4. Results

4.1 Chemical and spectral analysis

Field samples represented two areas in the ashes dam. From a total of 10 samples, 5 were collected at the eastern extreme of the ashes pond and the other 5 at the opposite side (fig 3.4). Both set of groups share similar components such as jarosite, gypsum and quartz. The first set of samples are also composed by other minerals such as starkeyite, copiapite, and rozenite which its presence suggest a more acidic environment than the other set of samples. Appendix 1 shows detailed information of the main components of each field sample according to XRD analysis results.

When analyzing laboratory and field spectra from the field samples, the minerals visually identified in these reflectance spectra were also indentified as major components according to XRD results (fig 4.1). Samples were mixtures of components so special attention was drawn to absorption features and curve shapes (appendix 2) to recognize tailing related minerals. Figure 4.2 presents a mixture of jarosite and goethite that can be distinguished in the lab spectra of samples 14, 15 and 16.

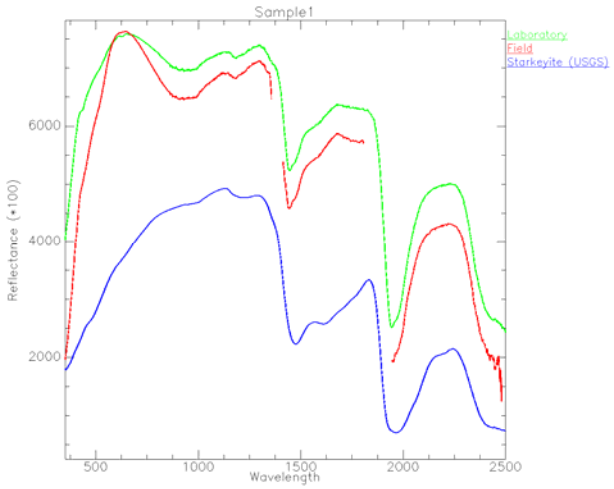

Figure 4.1. Reference spectra for a mineral found in field, and laboratory spectra of sample 1.

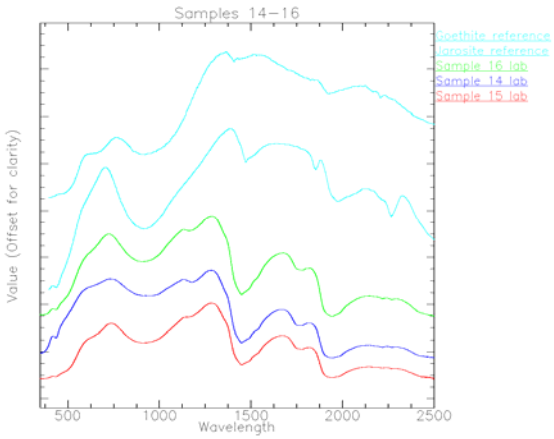

Figure 4.2. Example of mixture of elements found in samples 14, 15 and 16.

4.2 Processing of datasets

Once the images were atmospherically corrected and collected spectra processed, validation targets were used to compare image and field reflectances (fig 4.3). For all validation targets, image and field measurements are within 5% difference in reflectance for all wavelengths. The empirical line correction did not significantly improve the results, the multiplicative factor calculated from the calibration targets as the ratio between the image spectra and field spectra was also within 5% difference (fig 4.4), therefore it implies that this percentage is considered to be acceptable and the atmospheric correction run satisfactorily.

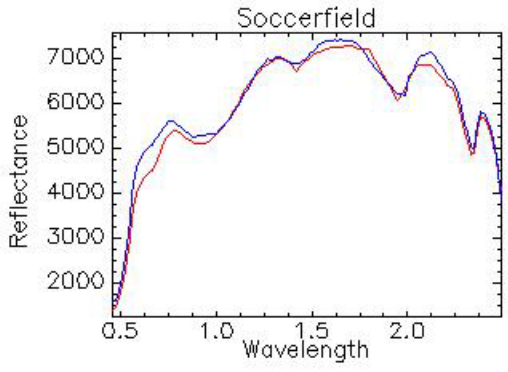

a

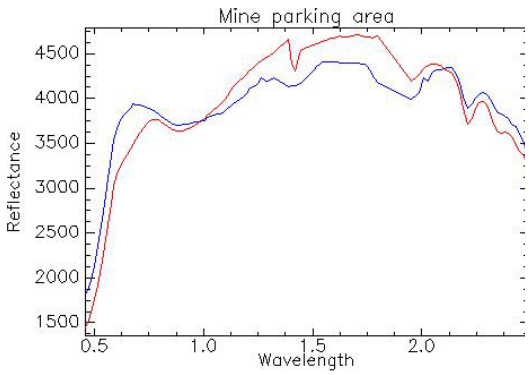

b

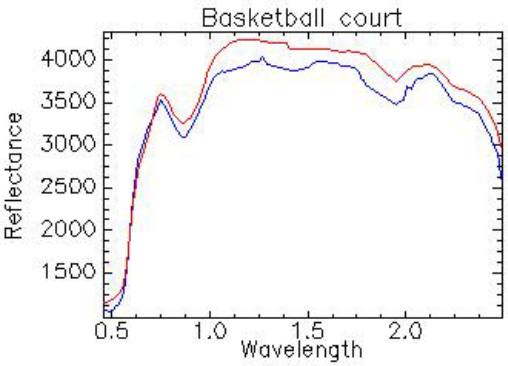

c

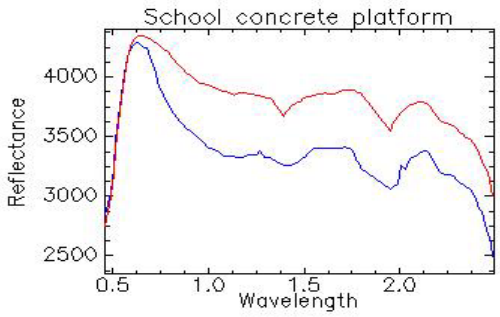

d

Figure 4.3. Spectra obtained from calibration target from field measurements Hymap image Field data ssed Hymap image, 2008. Units: reflectance in [% * 100]

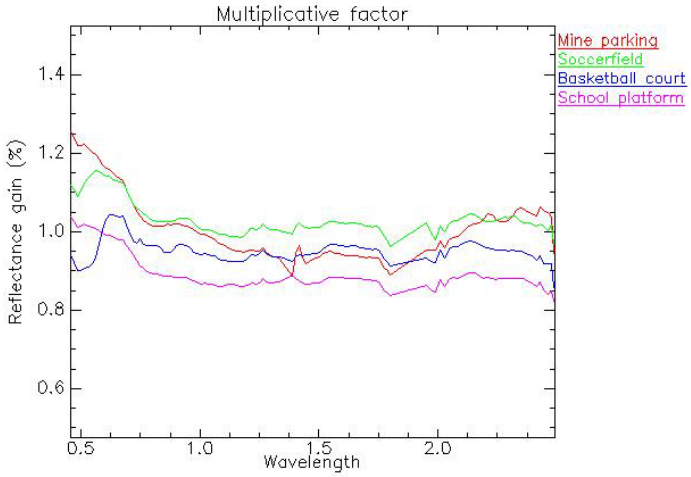

Figure 4.4. Multiplicative factors of an additional empirical line correction. Values calculated as the ratio between image and field spectra.

Calibration targets overlapping from different flight lines presented similar reflectance (fig. 4.5), so even though there was no ground data for 2nd or further scene/flightline, all the images corresponding to 2008 are spectrally coherent.

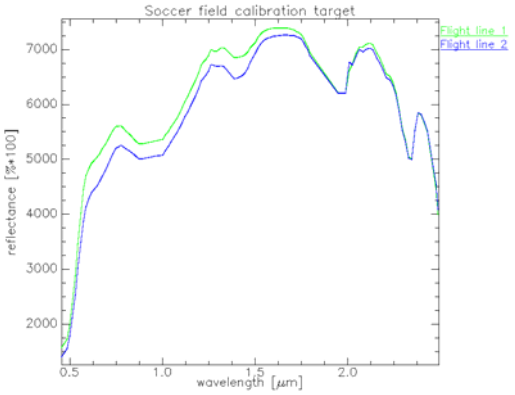

Figure 4.5 Calibration target spectra from two different flight lines of 2008.

Figure 4.6 compares the spectra of a calibration target (mining parking lot) for 2004 and 2008. From this validation it could be concluded that the differences between spectra were no more than 5 % percentage absolute for all wavelengths. Additional tests with other invariant surfaces support these finding. Therefore the 2004 and 2008 images are spectrally similar and could be use to map change detection.

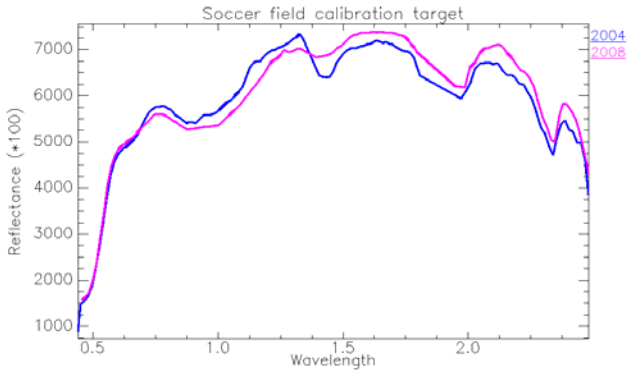

Figure 4.6 Spectra of mining parking lot for 2004 and 2008.

4.3 Mineral mapping

4.3.1 Tailing related endmembers

Endmembers extracted from the mine-tailing areas were different than in the surrounding areas, therefore this region presented unique mixture elements that are related particularly to these areas. This phenomenon occurs for both years. Figure 4.7 illustrates for the tailing area in 2008, how a spectral library with endmembers associated to the tailing area, has a different frequency distribution if they are used to map the tailing area or the tailing area and its surroundings.

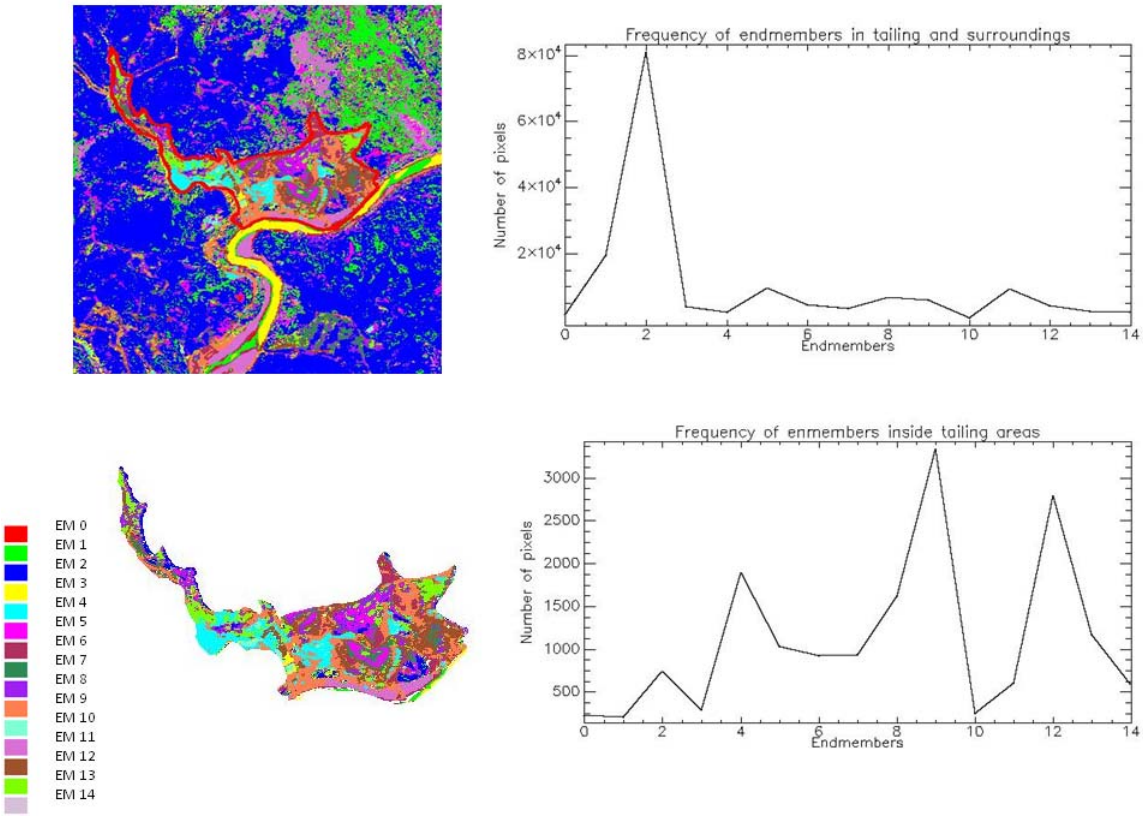

Figure 4.7. Illustration of endmembers used to characterize tailing area in 2008. Comparison of changes in frequency when endmembers are used to map only the area inside the tailing or its surroundings.

4.3.2 Mineral mapping method

SAM and MESMA showed similar results reflected in congruent distribution of spectral patterns. A confusion matrix (table 4) was performed to compare the similarity of both mapping methods giving 72% and a kappa coefficient of 0.62. According to this matrix endmembers with the lowest performance were He-Go_27 and Ha-Co_20. He-Go_27 is confused with He_68 and Ha-Co_20 with Ro-Ha_22. For both cases, errors in the classification are between other endmembers containing the same mineral, therefore it could be a matter of differences in mixtures of spectra and labeling of endmembers. Since the predominant mineral is recognized in both cases the results from both methods are similar. When comparing mineral maps (figure 4.8) SAM seems to be less scattered and more spatially coherent than MESMA. Therefore the final characterization of the tailing and mining areas were performed using SAM.

Table 4. Confusion matrix comparing results of mineral characterization using SAM and MESMA method for tailing area in 2008

		SAM							
	CLASS	Co_82	He-Go_27	Ja-Go_17	He_68	Ro_3	Ro-Ha_22	Ha-Co_20	Total
MESMA	Co_82	91.89	0.59	5.4	0	0	0.85	0.44	2.89
	He-Go_27	5.41	65.3	4.59	4.85	0	0	0.44	22.63
	Ja-Go_17	0	0.66	71.72	10.79	0	0	3.41	34.22
	HE-_68	0	33.41	14.56	83.98	0	0	0	28.9
	Ro_3	0	0	0.02	0	96.76	9.97	5.71	1.83
	Ro-Ha_22	2.7	0	1.27	0	3.24	89.17	20.11	4.02
	Ha-Co_20	0	0.05	2.44	0.38	0	0	69.89	5.52
	Total	100	100	100	100	100	100	100	100

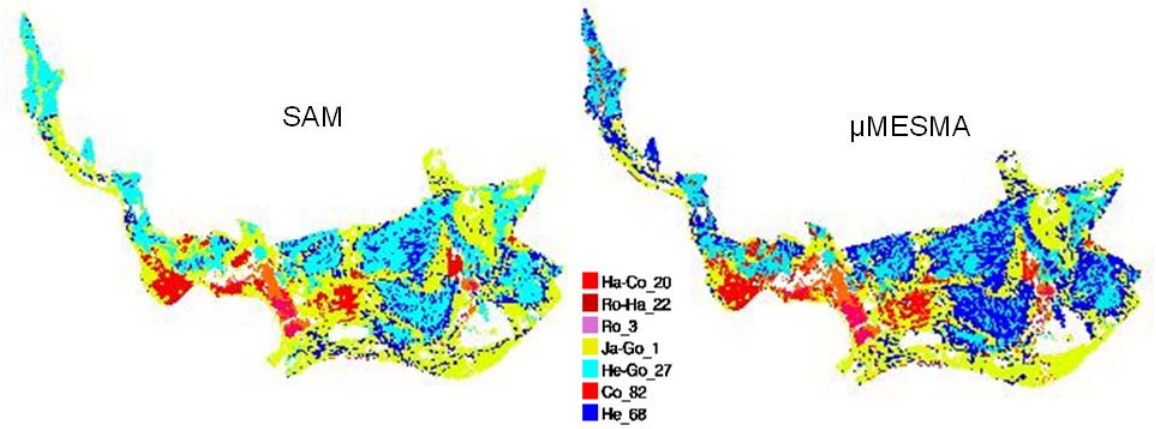

Figure 4.8. Mapping results of tailing area in 2008 using SAM and μMESMA. Similar spectral patterns are recognized but SAM seems to show less scattered results.

4.3.2 Endmember identification

Endmembers were not pure elements but mixture of spectra, so it became a challenge to determine tailing related spectra when compared strictly to the spectra references. Important absorption features and the shape of the reflectance curve helped to determine the presence of certain minerals and mixtures of them. The main minerals

identified were hematite, goethite, jarosite, schwertmannite, rozenite, halotriche and copiapite. Figure 4.9 shows mixtures and variations of these minerals extracted from tailing and mining areas from both years.

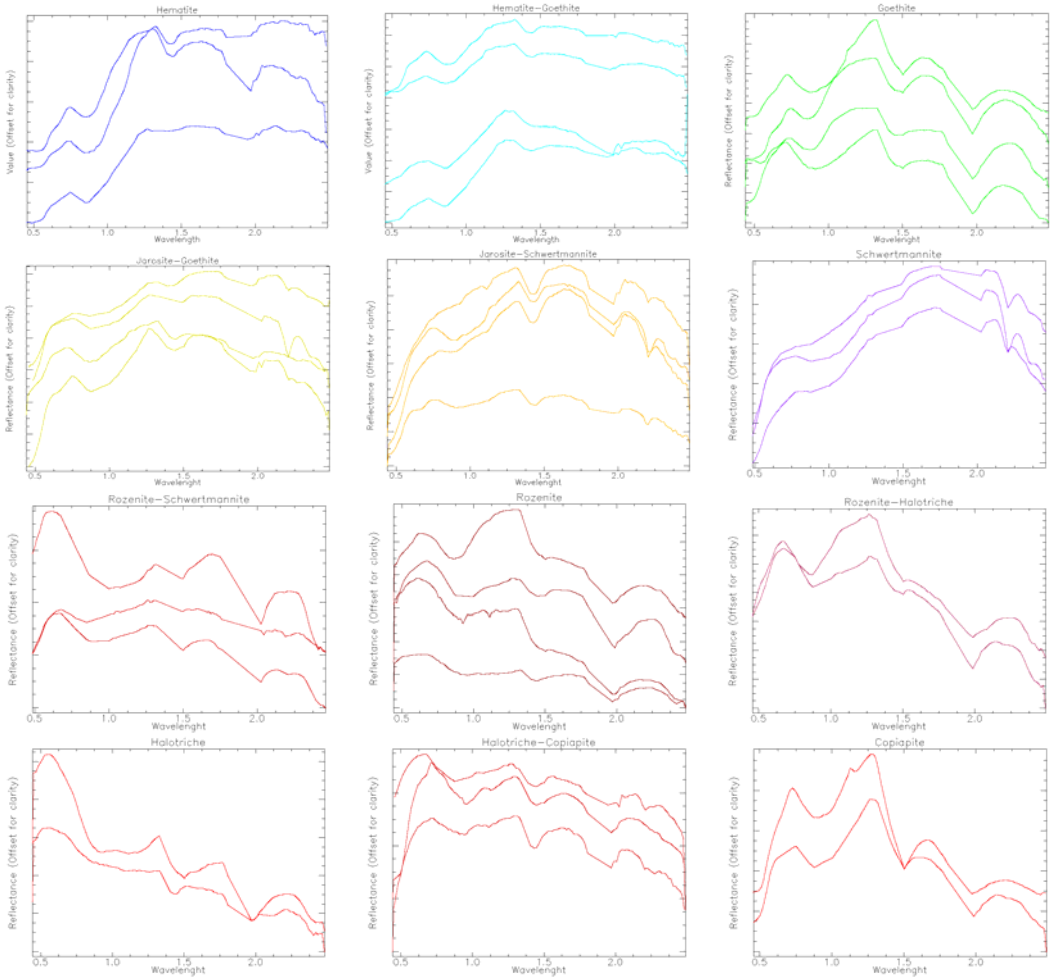

Figure 4.9. Endmembers from mineral spectra libraries labeled according to predominant minerals. Extracted from tailings and mining areas, from 2004 and 2008,

The following section provides a description of mineral mapping results for the two areas of interest. Figure 4.10 shows the main components of minerals identified in the extracted endmembers and the colors, in which they are displayed in the maps.

Figure 4.10. Color display for minerals labeling in mineral maps from tailings and mining areas from 2004 and 2008.

4.3.4 Mineral maps

Tailing area

The area refered as tailing area is located next to the river Odiel. Its geographic location is downstream of the watershed and three river afluents cross this area before reaching the river. This area hasn't been rehabilitated. Similar distribution patterns of spectral clusters composed with hematite surrounded by goethite and jarosite can be observed in both areas, as well as presence of rozenite, halotriche and copiapite. When comparing results from both year in a general way it can be said that there hasn't been drastic changes over 4 years. The dominant mineral types are the same and the area where they occur also show a similar pattern size. But there are two important transitions that can be noticed, the presence of spectra identified as hematite inside clusters of hematite-goethite and an increment in the variety of efflorescense salts such as rozenite, halotriche, and copiapite (Figure 4.11).

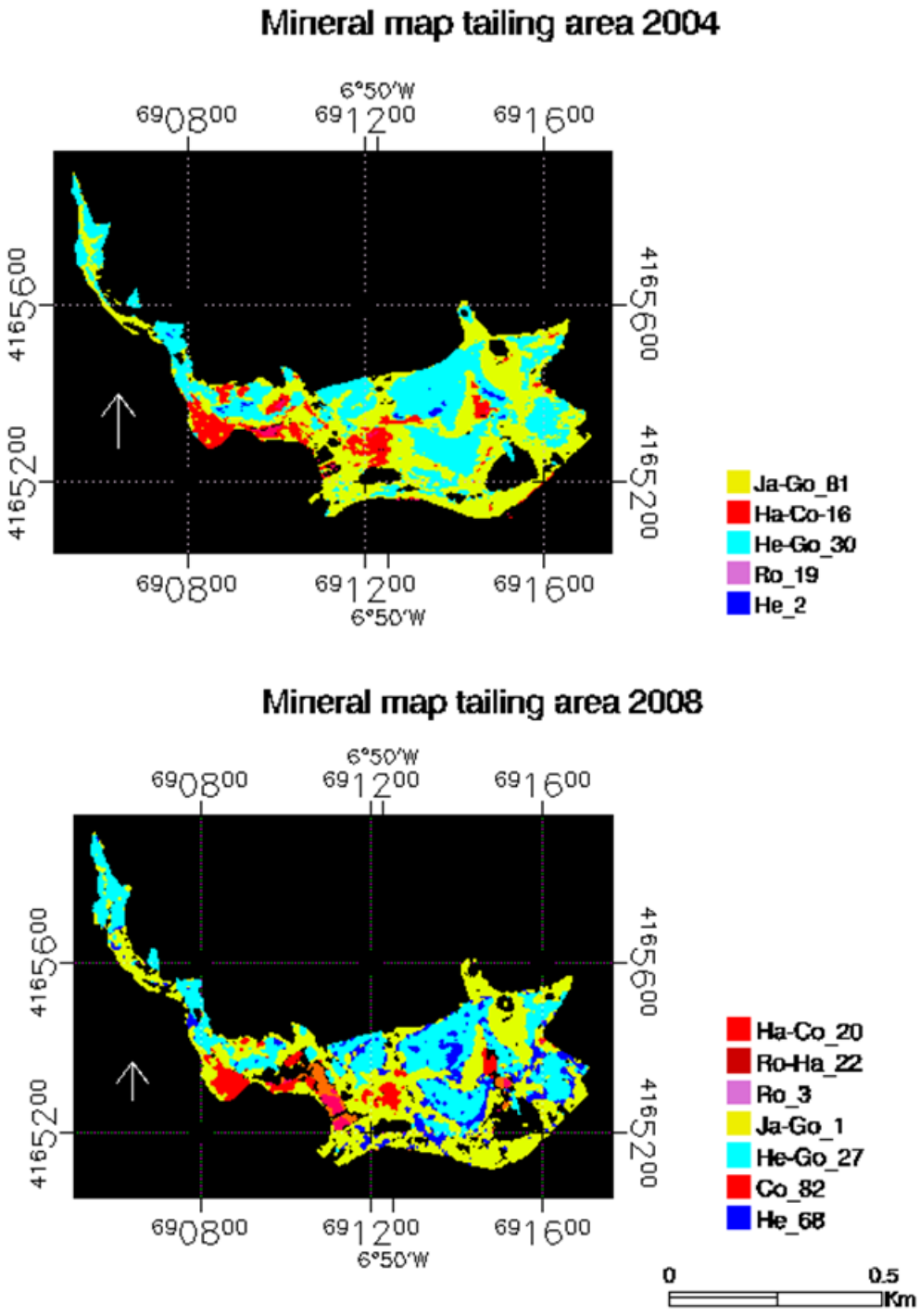

Figure 4.11 Mineral maps of tailing areas from 2004 and 2008.

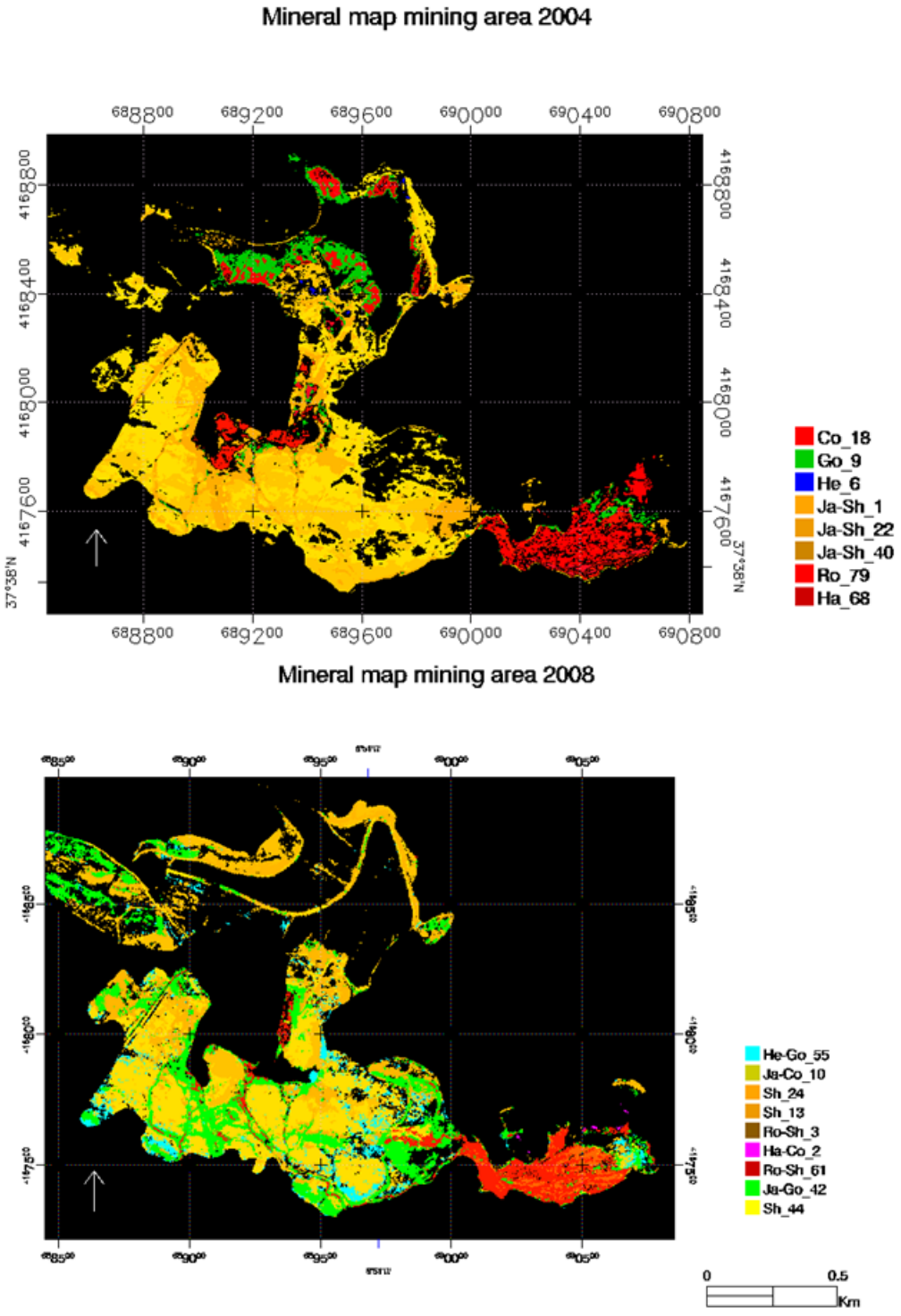

Figure 4.12. Mineral maps of 2004 and 2008 of mining area.

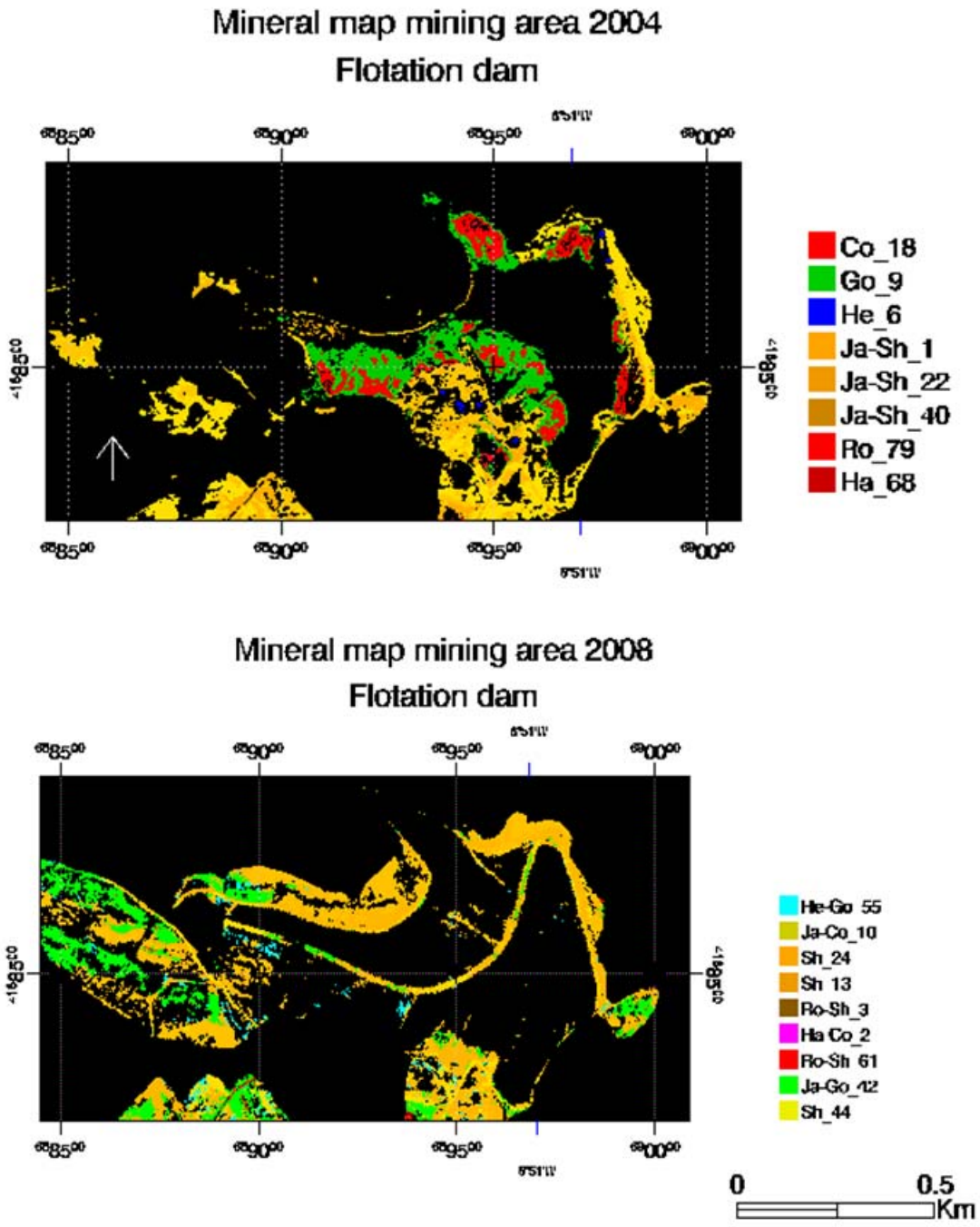

Figure 4.13. Mineral maps of 2004 and 2008 of mining area. .Enlargement of flotation dam

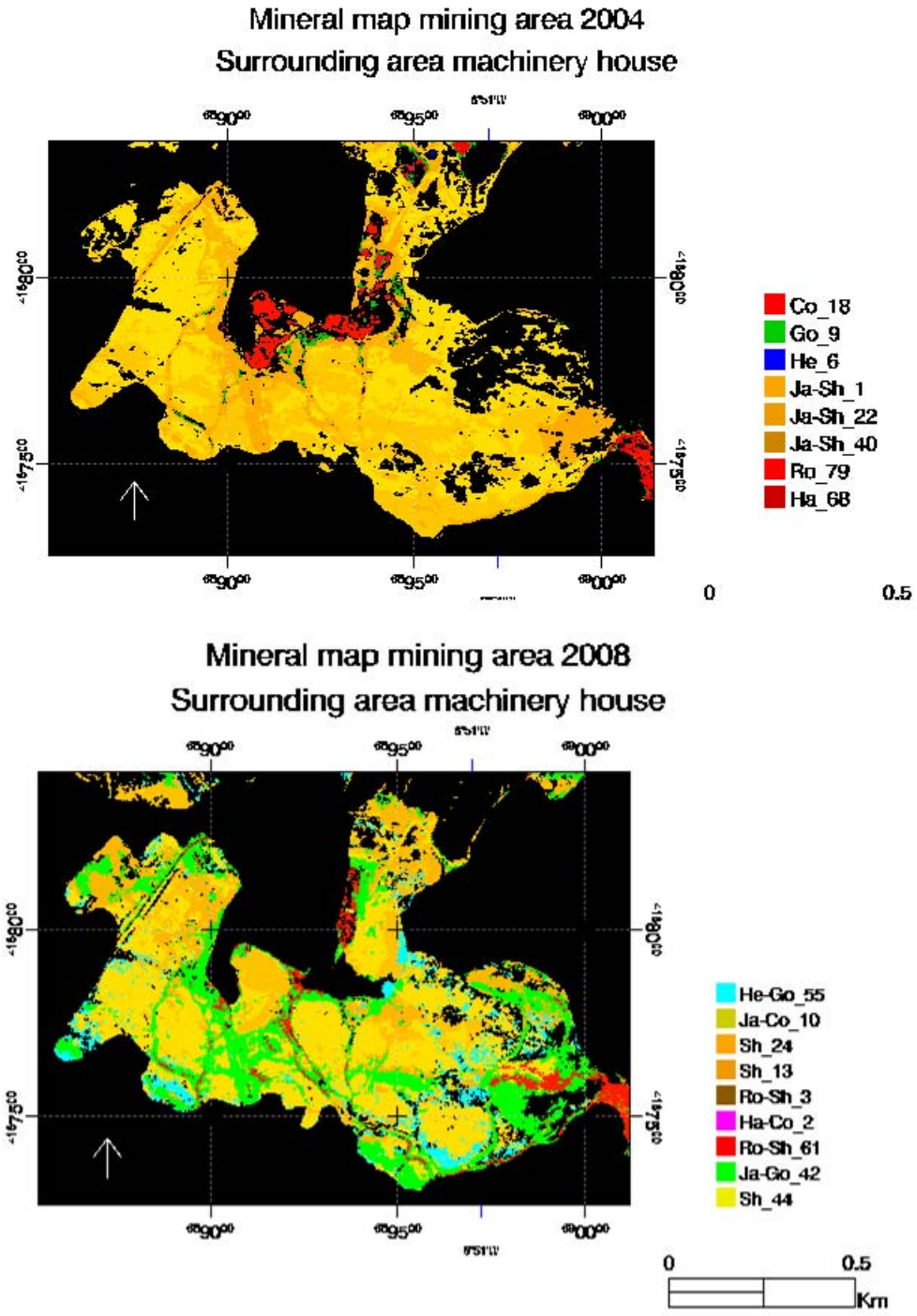

Figure 4.14: Mineral maps of 2004 and 2008 of mining area. .Enlargement of surrounding area of the machinery house.

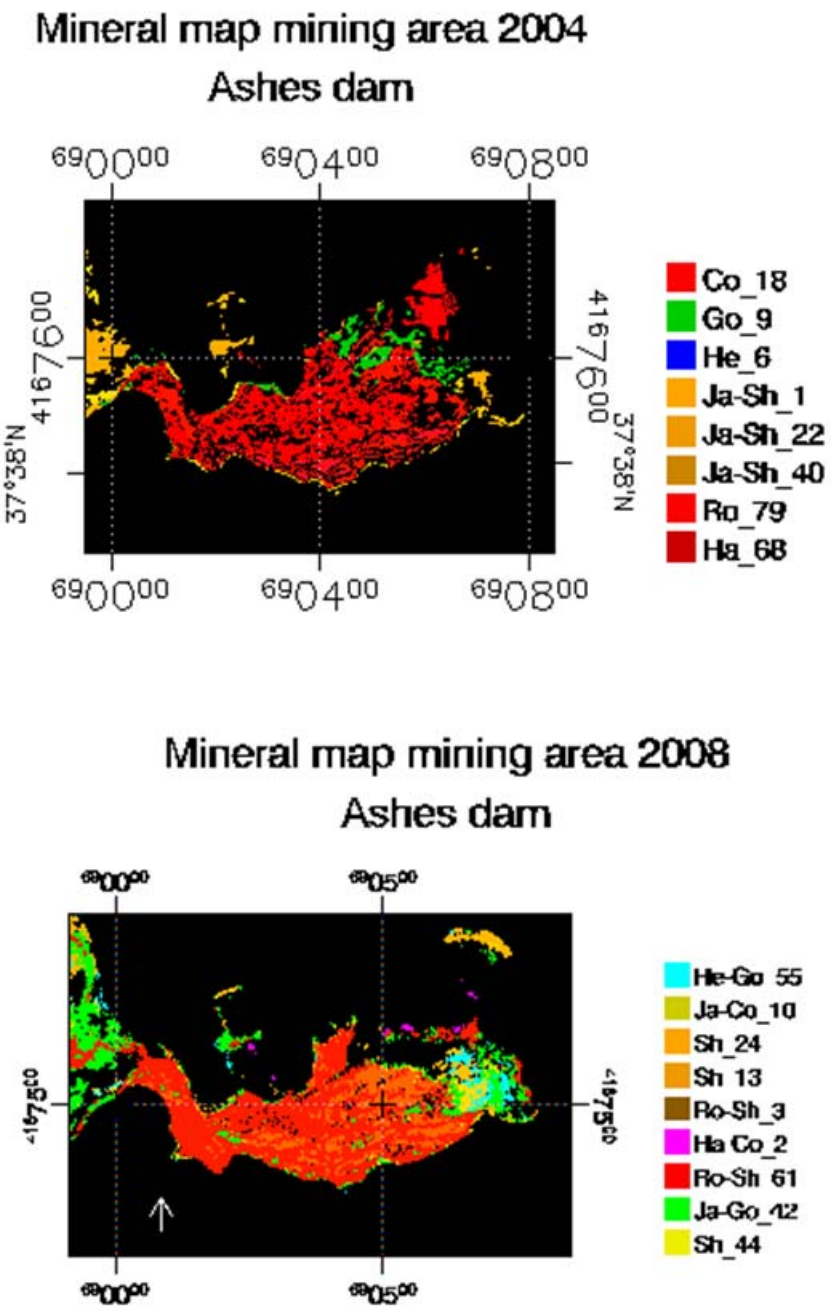

Figure 4.15: Mineral maps of 2004 and 2008 of mining area. .Enlargement of ashes dam.

Mining areas

The mining area is being rehabilitated. This process has been done by phases and the results portray the mineral composition from both years (figure 4.12). The description of this area is performed by characterizing the flotation dam (northern dam), which by 2008 had been filled up, sealed and covered with vegetation The second area described is the surroundings of the machinery house and finally the mineral composition of the ashes dam is detailed. Descriptions of these areas are detailed below.

Flotation dam

This area is the northeast dam and presents the most drastic changes (figure 4.13). Rehabilitation measurements are recognizable. Areas not mapped in 2004 correspond to water inside the dam, areas not mapped in 2008 are because the spectra is no longer recognized as tailing related minerals but as dry vegetation. Efflorescent salts (halotriche, copiapite, rozenite) are not present in 2008 but there is an increment of minerals at the western edge of the dam where jarosite and goethite are detected. At the opposite side of the dam, there is a small area at the eastern side, that in 2004 jarosite was predominant but in 2008 goethite is also present. This area is located down slope of the terrain were water runs from the dam into the open field.

Surroundings machinery house

When labeling endmembers, a mixture of jarosite and schwertmannite seemed to be predominant in 2004 (figure 4.14). Instead of grouping this endmembers together they were kept separate and colored with a variation of yellow-orange colors so the spectra structure of the area covered with some amount of these minerals was still visible and possible to differentiate. If they were grouped together different spatial patterns would have been lost. In 2008, some of the darker yellow marked areas in 2004 seems to change into mixtures containing goethite. Red minerals are spotted in a way that suggests to be following a water flow topology.

Ashes dam

Comparison of mineral maps from 2004 and 2008, reflect the main changes this dam has gone through the last 4 years (figure 4.15).. Even though they are not as drastic as the flotation dam, this dam belongs to the second phase of rehabilitation procedure performed by EGMASA (section 3.1.4). Areas not mapped in 2004 are because of the presence of water. Image of 2008 shows the dam as a solid area of efflorescent salts, confirming that the mine is being dried out as stated in the management plan of the rehabilitation process.

Water is still contained at the eastern edge and the mud around presents a variety of minerals different from the rest of the dam covered mostly by rozenite and schwertmannite.

4.4 Boundaries delimitation

Richter's (2004) study was based in Kam Kotia mine in Ontario, Canada. Even though the climate and location of both study sites are different the methodology of how the boundaries were defined was tested for the Sotiel Migollas imagery. As stated in section 3.3.2, boundaries delimitation method as proposed by Richter (2008) could not be applied. The main reasons are because the transition areas between vegetation and other land uses were not as crisp and clear as in Canada , and also because this study implies time series analysis so the definition of boundaries should apply to both datasets in order to compare them properly. Image of 2004 was taken in May during Spring season but the one of 2008 was taken in August during Summer period. Therefore areas mapped as changes were going to detect seasonal changes and not tailings which is the main objective.

In figure 4.16 the abundances map from Kom Kotia mine in Canada and Sotiel Migollas in Spain are compared. First a false color composition of both sites, from Spain for both years, gives a hint in the differences of vegetation cover between both countries. In Canada vegetation is condensed and much differentiated from the tailing area. In Spain, only for the image of 2004 there is some difference between vegetation and tailing, for 2008 vegetation cover decreases and is scattered over the entire area. The following images described the abundances per pixel for each spectral library used, in this case green vegetation, dry vegetation and minerals and soils.

The blue cover over 2008 indicates that green vegetation compared to 2004 in Spain has diminished. Even if there is more coverage of green vegetation in 2004, the abundance is not enough to fulfill Richter's requirement of 80% vegetation abundance to be consider as green vegetation coverage. Dry vegetation and tailing related abundance maps are also not as clear in Spain as they are in Canada. In Canada dry vegetation occurs in the transition area between the tailings and green vegetation coverage. Dry vegetation in Spain, occurs all over the study region and there is an increment of abundances in the image of 2008 due to the dry season. Tailings areas are noticeable for 2004 in Spain, but for the image of 2008 image it is not possible to differentiate tailings based on abundance coverage since all the area presents an homogenous abundances of minerals- soils endmbembers with no differentiation of the mine area for example.

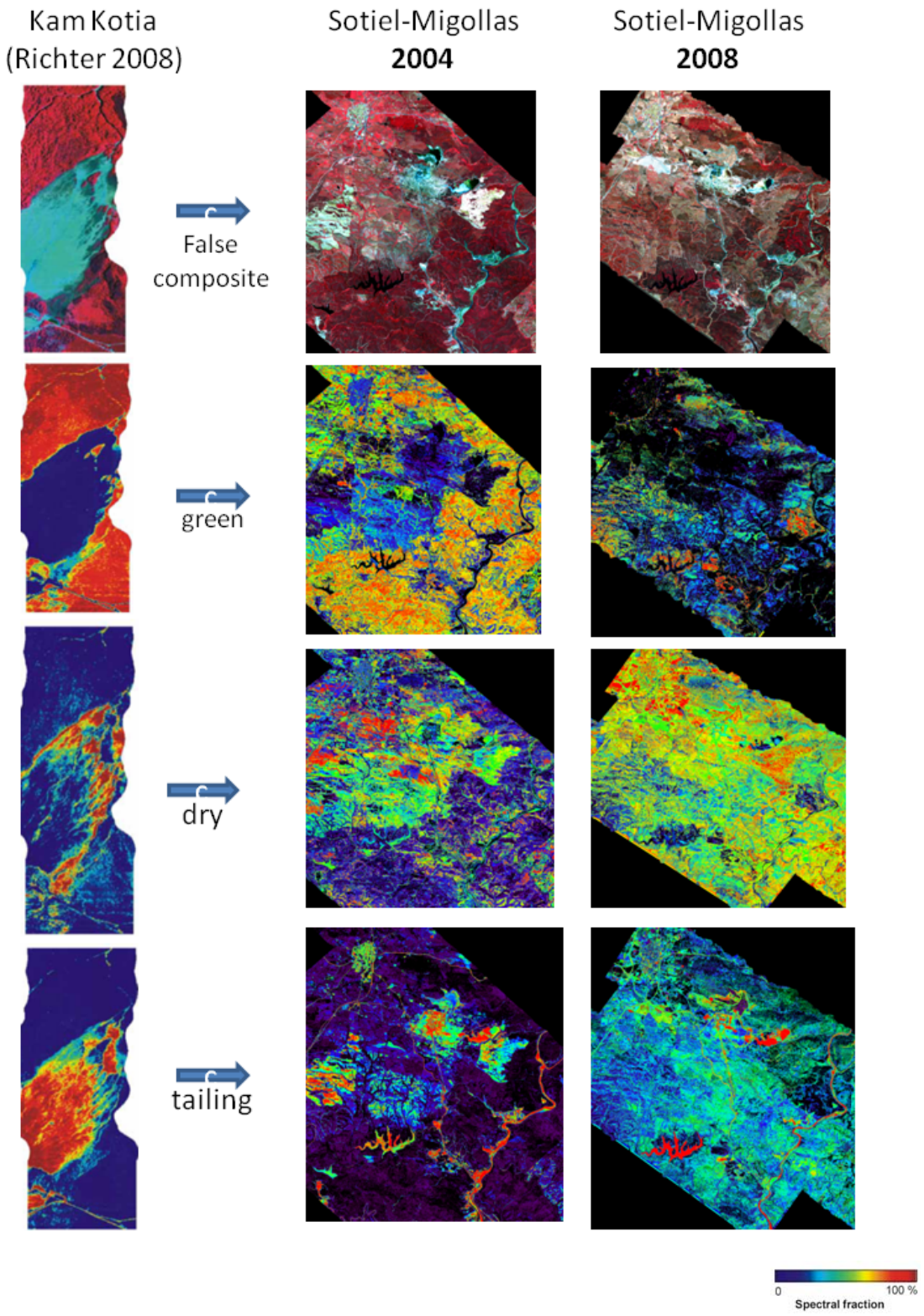

Figure 4.16 False color composite of Kam Kotia mine in Canada, Richter (2008) and respective abundances of green, dry vegetation and soil and minerals in Sotiel Migollas mine in Spain. Regions in blue color have no cover of its respective material whereas region with red color indicate full surface cover.

An alternative to define boundaries delimitation, as, suggested in section 3.3.2, is based on the images frequency statistics and calculates the threshold by adding the mean abundance value of the mineral areas plus one standard deviation. This method was applied to whole the study area. As depicted in figure 4.17, this method seems to delineate the mining area in the image of 2004. For 2008, areas around the machinery house that were mapped in the mineral characterization method were not classified as tailing area. Another challenge faced when applying this method, was that in 2004 there were two clearcut areas affected by a fire and classified as tailings. In the image of 2008, these areas seem to have recovered but the classification is scattered around this region. It may have been possible that the mineral spectral library of 2008 was not properly characterizing endmembers related to tailings. The subset area where mineral characterization was performed corresponding to the tailing area, was mapped using very well defined spectral libraries. Therefore this method was tested in this data set for both years. The method seems to define properly the tailing boundaries for 2004 but for 2008 there are some gaps in the center of the tailing area and results seem scattered over the area (figure 4.18).

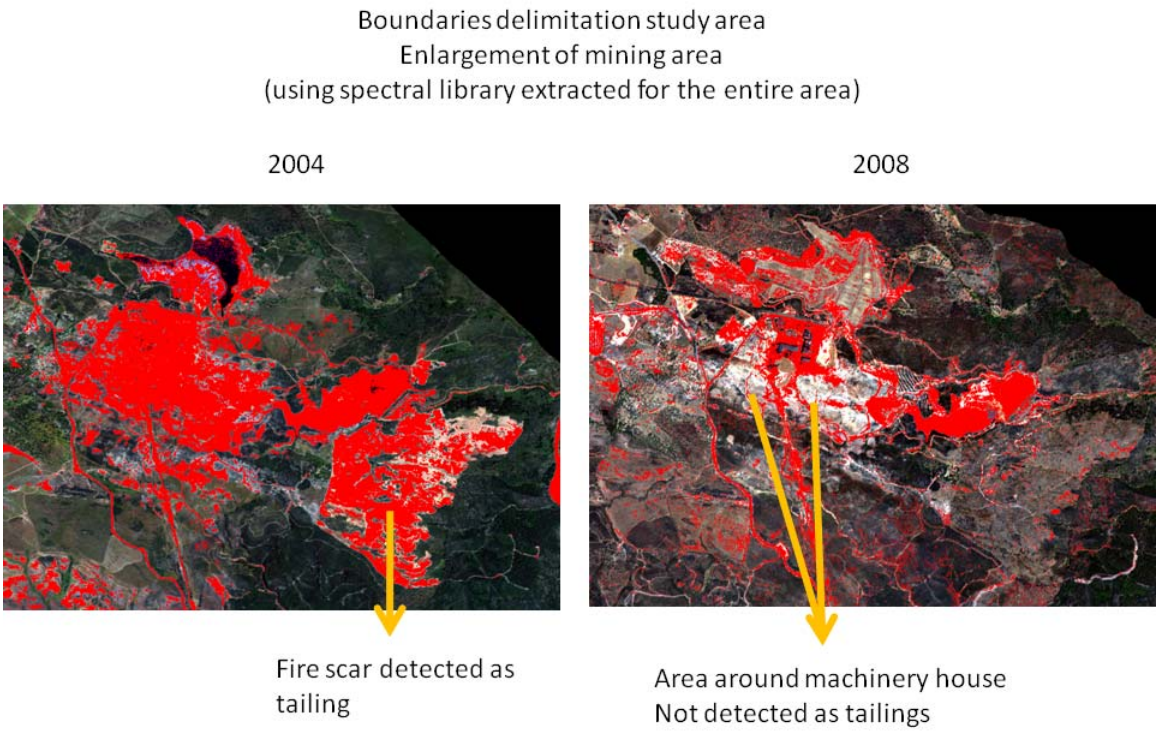

Figure 4.17: Tailings boundary delimitation (red area) in study area for 2004 and 2008. Enlargement of mining area.

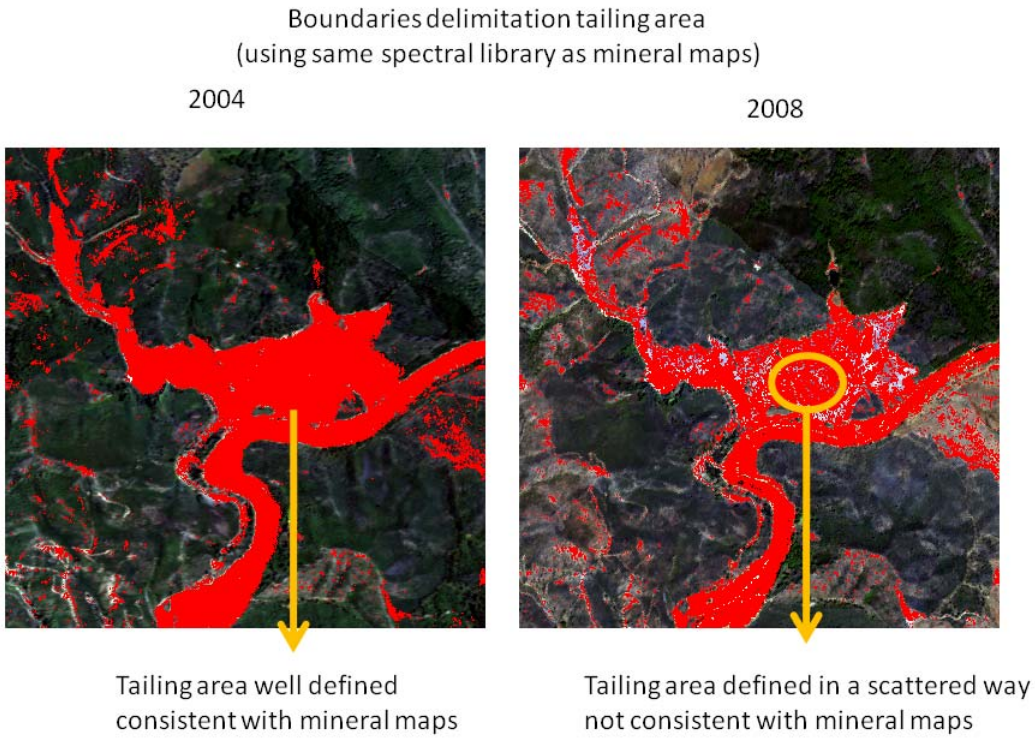

Figure 4.18: Tailings boundary delimitation (red area) in tailing area for 2004 and 2008.

4.5 Validation of mineral maps and boundaries delimitation

The assessment of mineral maps and boundaries delimitation, as explained in section 3.3.3, consist of comparison of 2004 mineral map results from Zabcic (2008), XRD results from 2008 and cross checking results from both methods for both years. Zabic (2008) produced mineral maps of the mining area and tailing area, using a similia linear spectral unmixing approach (ISMA), that presented the same spectral pattern and similar composition of minerals as the one presented on this study (figure 4.19). That research involved exhaustive field campaigns where over 100 samples were collected in the field and analysis of XRD were performed. Endmembers labeling contain different mineral composition since they were named after XRD results, but al least one of those minerals were found in endmembers labeling from this study. This indicate that the results of 2004 from this study and Zabcic (2008) are comparable and therefore similar.

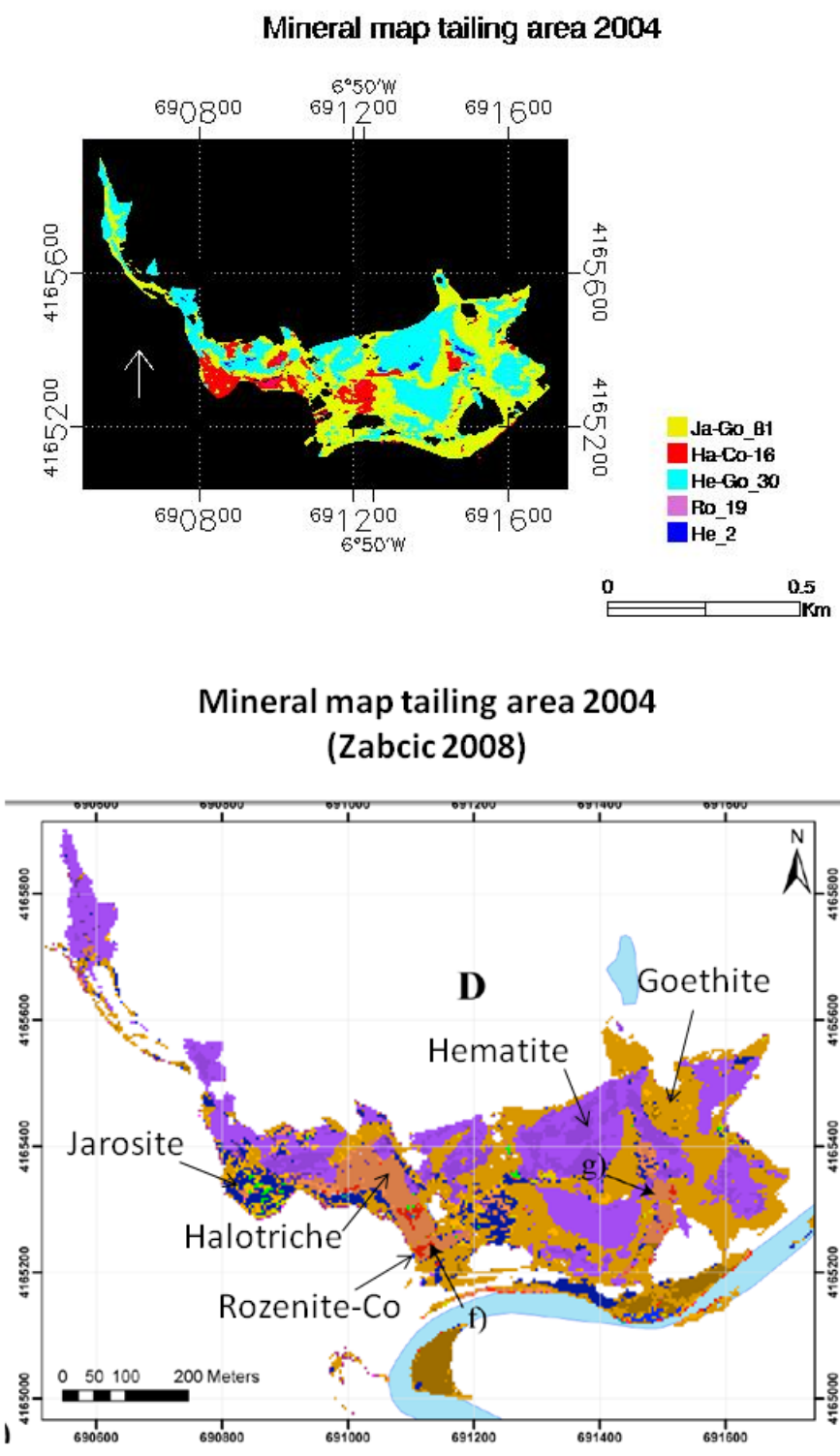

Figure 4.19. Comparison of results from this study and Zabcic (2008) for the tailing area in 2004. Similar distributional patterns are recognized in both maps and results are classified using the same endmembers labeling.

Field samples from 2008 were collected from two different areas of the ashes dam. As detailed in appendix 1, XRD results present similar composition of minerals for all field samples, but the presence of starkeyite, rozenite and halotriche in the ones collected at the western side of the dam (samples 1-5) presents more acidic conditions that the other group of samples collected at the northern edge of the dam (samples 12-16). The presence of goethite is a hint that the later region region is more advanced in the pyrite oxidation cycle. The maps of 2008 reflect the same situation as the XRD results (figure 4.20). Since samples were not collected within a significant distance from each other, the comparison consider samples taken at each site as a whole. This is confirmed with the fact that the mineral composition of the samples is similar and that spectra from the image is homogenous in most of the dam. The presence of goethite detected in the samples from the northern edge, agrees with the few pixels detected at the edge of the dam colored green.

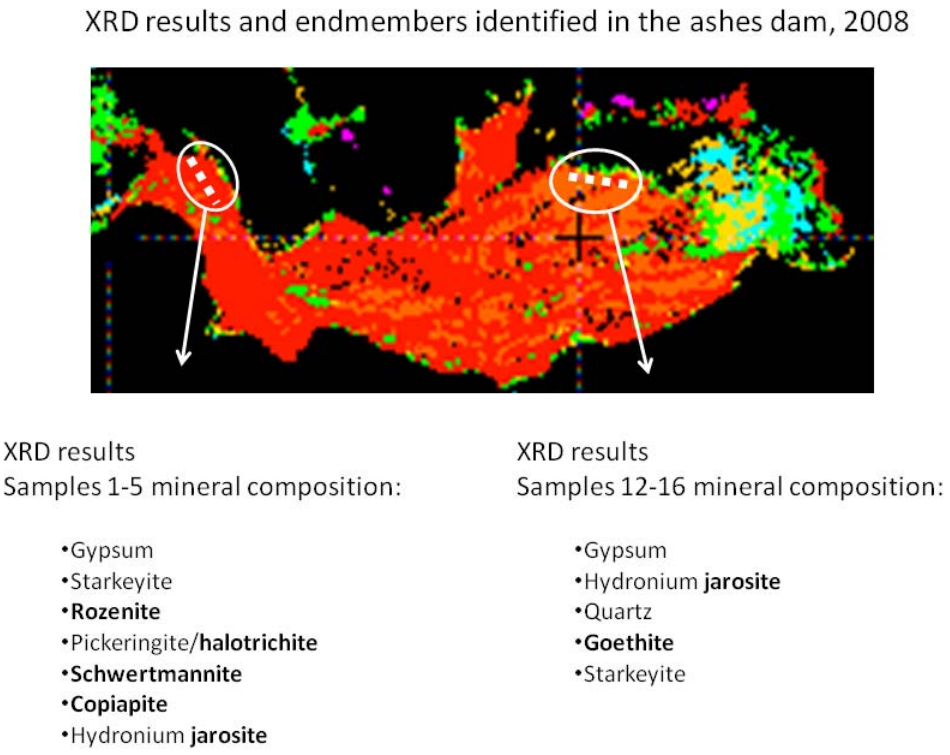

Figure 4.20. XRD mineral composition for field samples collected in 2008. White dotted line (not scaled) indicates the sites were sample 1-5 and 12-16 were collected in the ashes dam. Minerals found in XRD results and marked in bold are also found when labeling endmembers spectra extracted from the image of 2008.

Cross verification analysis consisted in a visual comparison between mineral maps and boundary maps obtained from each year, this to ensure that results were congruent and consistent with each other. As described in section 4.4, maps obtained from 2004 retrieved similar results than the ones from 2008 Figure 4.21 illustrates this case for the surrounding area of the machinery house of 2008. Area defined as tailing by the boundary delimitation method did not correspond to the areas characterized as tailing related minerals obtained from the mineral maps. Therefore another approach was performed in the subset tailing area and the results for 2008 visually improved between both methods (figure 4.18).

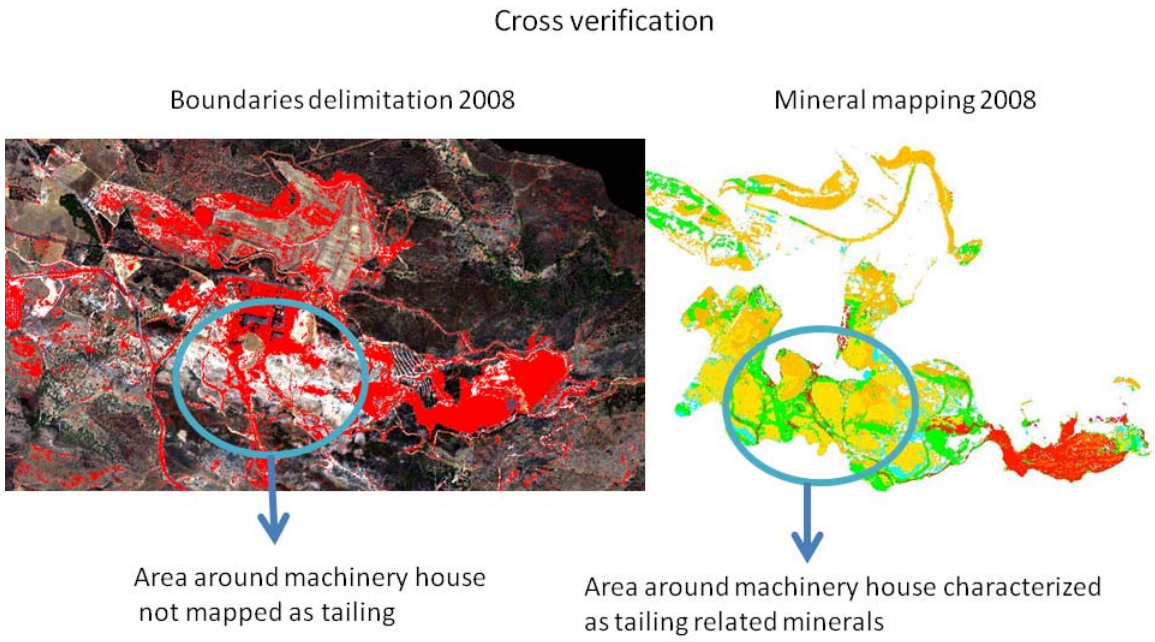

Figure 4.21. Cross verification of boundaries delimitation results and mineral mapping for 2008. Area defined as tailing by the boundary delimitation method did not correspond to the areas characterized as tailing related minerals obtained from the mineral maps.

Chapter 5. Discussion

The results obtained in this study are showing two important aspects of mining environment. One aspect is the monitoring of a mine after remediation efforts have started, as was described for the mining area; and the second aspect is the monitoring of an area left abandoned without any remediation actions reflected in the tailing area. Assessments of the two sites and discussion of the application of each method is described as follows.

Mineral mapping

The tailing area served as a deposit of waste rocks next to the Rio Odiel. As shown in the results section (figure 4.10), the area is not presenting drastic changes in the last 4 years in terms of size and mineral composition. Nevertheless some areas seems to be in a transition of becoming more neutral and other are in early stages of the oxidation process, such are the areas where rozenite, halotriche and copiapite are recognized. The pattern where this minerals are located suggests that they are following the course of waterflow that runs through the tailing.(appendix 4). The pattern of hematite surrounded by goethite and further on with jarosite as well as the cluster of efflorescent salts close to jarosite suggested a similar pattern observed at the California Gulch Superfund Site in Colorado by Swayze et al. (2000). Jarosite and efflorescent salts are located at lower elevation than the surrounding slopes of goethite and hematite. Runoff from the tailing drain into the lower levels produce an accumulation of AMD in these pools that eventually cause the precipitation of efflorescent salts and drainage of them into the river.

The rehabilitation process of the mining area is performed in two separate phases, the first one is already accomplished and the second one is taking place. During the first stage the flotation dam was dried, filled and sealed, and this procedure is reflected in the map obtained for 2008 (figure 4.12). This area presents the most drastic changes. In 2004, it presented all the conditions of a focus point of AMD producer with minerals at an early stage of the pyrite oxidation process. For 2008 most of the area is not identified as tailing but as dry vegetation and soil. It would be interesting to monitor the vegetation in the flotation dam in spring or by means of soil samples., To measure if vegetation recovering is successful and if the soil quality at the top layer is good enough for vegetation recovering. Since the image was taken in August, it is not clear if the attempt of covering the area with grass is successful and was dry because of seasonal effect or if the top soil conditions are not appropriate for re-growth of vegetation. The surroundings of the mine still have some evidence of jarosite and goethite, it may be caused by the movement of materials from the restoration steps. Although the presence of jarsosite indicates that the sourroundings of the flotation dam is not yet stable, presents a more advance oxidation stage than in 2004.

Part of the first stage in the rehabilitation of the mine is the removal of mine installments, therefore the surroundings of the machinery area presents changes (figure 4.13). The most evident is a transition towards a neutral stage although the presence of jarosite and goethite still has to be treated. In the image of 2004, spectra classified as schwertmannite presented a vast variety that if grouped together the distribution of spectral patterns was lost. They were maintained separately and differentiated. For 2008, some of these variations of schwertamnnite (darker yellow variation) is the one being recognized in the next image as a transition to goethite and hematite. There is still significant presence of jarosite and formation of efflorescent salts is noticeable at the eastern extreme where the ashes dam starts

The ashes dam is undergoing rehabilitation process and the image of 2008 reflects this (figure 4.14). There are areas not mapped in 2004 due to the presence of water, in 2008 this regions are characterized as halotriche and rozenite. The area close to the surroundings of the machinery house presents more acid conditions than the opposite side close to water still left.. At the edges of the dam the presence of goethite recalls some neutralization at the most dried areas. Due to the fact that this mine is being dried for the next restoration steps to take place, it could be illustrating the process of AMD production in a more accelerated way than it will occur under normal weather conditions. No more wastes are dumped in these dams and water is drained, so there is a gradient of areas that still have some water but haven't dried out completely like the eastern side. In 2004 some of this regions was not sensed because they were covered in water but in 2008 since its dryer its exposition with oxygen increase the rate of sulphide oxidation. The presence of rozenite indicates low relative humidity. The area closer to the water presents a diversity in mineralogy indicating that the oxidation of pyrite is still in progress and the tailings are not stable.

The results discussed show that topography plays an important role in the distribution of secondary minerals displaced by the surface runoff. In addition of providing locations of acidity and guidance for sampling collection, they also provide an overview of the implementation of rehabilitation procedures an its main effects as well as an indication of more sensitive areas for future remediation efforts. The maps offer an insight of the oxidation state of the entire site, this information is valuable for taking actions in case of climate or weather variations, for example heavy rains.

The main challenges when applying this methods relies in the labeling of spectral endmembers. The combination of XRD results with spectral references to label endmembers is an ideal combination. Even though XRD analysis does not always give accurate identification of the mineralogy of the samples it offers a guidance when using

spectral references to label endmembers. XRD results are not always available and the majority of endmembers have to be labeled by means of careful visual interpretation. of spectra absorption features and reference spectra. This method remains very subjective, specially since the reference data refers to pure minerals and very often the endmembers refers to mixtures of materials.

Boundaries delimitation

The method of boundaries delimitation could not be applied as suggested by Richter (2008). The way to define threshold to delineate boundaries according to Richter was by the percentage coverage of vegetation in combination with dry vegetation and minerals. The images for Sotiel Migollas were taken during different seasons therefore the classes that define changes by Richter , in this study are going to define changes in seasonality which are no changes caused by tailings. The study area of Richter was also more homogeneous than this study area, where cities and agriculture land were also included. An important observation were fires detected as tailings in 2004 and some of this areas were already recovered in 2008. So the classes defined by Richter were no sufficient to characterize the mining surroundings and its affections in this study area. The new proposed way to delimit boundaries thresholds was obtained after considering vegetation and dry vegetation as a combined class and areas not included in this criteria as tailings.

Furthermore, it is suggested a way to define boundaries delimitation thresholds based on the statistics of each year and not on static percentages. The definition of a threshold as the mean abundance value of the mineral abundance maps plus one standard deviation could be an useful method that can be applied to time series analysis. For this study area, this method retrieved satisfactorily results for 2004, but not for 2008. This could be because of lacking endmembers in the spectral libraries that feed the model. Running the model takes a lot of time and feeding it with minerals library with too many endmembers may result in errors. Therefore the method was tested in the tailing area, where the mineral spectral libraries were complete and well representing the tailing environment. The definition of the tailing boundary improved , although there are still areas for 2008 (figure 4.17) that are not identified as tailings even though they are located in the center of it. The reason of this confusion could rely in the classification of soil spectra in the mineral libraries. As shown in figure 2.3c, soils are a composition of different materials, minerals, organic matter, iron,etc. Because of the geology of the area it is possible that the top soil covering rock formations are dominated by iron and therefore classified as tailing related mineral. For future studies is recommended to differentiate between bare soil and mineral related endmembers. ,This can be achieved by a preselection based on absorptions features related to organic composition and clay matter and not only on iron bearing features.

To summarize, imaging spectroscopy is a useful tool for characterizing mining environments. The results from this study offer validation of rehabilitation efforts, guidance of areas that still need attention and offers an idea of the state of the mines that have similar characteristics as those of Sotiel-Migollas. As shown in figure 1, in the region of Huelva, Spain, there are many mines left abandoned and others at some process of rehabilitation. The results from this study can become handy as a guideline to describe what may be ocurring in other mines presenting similar conditions as described in these two sites.

There are still efforts to be made in improving models to monitor these environments, but in general the information retrieved presents valuable information specially to mine managers who usually do not have access to this type of remote sensing tools. As stated by Kennedy et al. (2009) it will be a both way benefit if mine managers are included with scientist in the development of these models. They could contribute with their field experience and at the same time they can understand the landscape dynamics over time., With this interaction models developed could be effective and fulfill expectations to achieve monitoring objectives.

Chapter 6. Conclusions

The objective of this thesis was to assess the opportunities to monitor rehabilitation development between 2004 and 2008 in the Sotiel Migollas mine according to methods derived from imaging spectroscopy, like mineral characterization and boundaries delimitation. Two main areas within the study region were analyzed and described: the mining area where rehabilitation measures had started and tailing area that is in an abandon state.

For the mining area, completed rehabilitation measurements have been monitored and reflected almost no coverage of tailings related minerals. Areas where there is still presence of tailing related minerals in 2008, are in a further stage of oxidation than in 2004. Abandoned tailing areas do not preset drastic changes in the period of four years, spatial patterns are similar through the years in its composition and distribution. Main changes are located where water runs off into the rio Odiel.

Mineral mapping characterization method presented several contributions for monitoring mining environments such as:

- support the role of topography in the distribution of secondary minerals
- guidance for sampling collection
- assessment of rehabilitation effects
- indication of sensitive areas for future remediation efforts
- overview of oxidation state of entire site

The main challenge regarding this method was the labeling of endmembers extracted from the images. The combination of XRD analysis and spectra references offers a good guidance for labeling endmembers. XRD results are not always available and the majority of endmembers have to be labeled by means of careful visual interpretation. of spectra absorption features and reference spectra. This method remains very subjective, especially since the reference data refers to pure minerals and very often the endmembers refers to mixtures of materials.

The method to delineate boundaries for monitoring expansion or reduction of tailing areas over the years, developed by Richter (2008), could not be applied to this study area due to changes in seasonality and land use dynamics of the region. A new method is suggested by defining tailing boundaries based on the statistics of each year and not on static percentages. The definition of a threshold as the mean abundance value of the mineral maps plus one standard deviation could be an useful method that can be applied to time series analysis. This method should be further studied with a complete set of mineral

spectral libraries extracted from the tailing areas and that presents no confusion with bare soil coverage.

Imaging spectroscopy is a useful tool for characterizing mining environments. The results from this study offer validation of rehabilitation efforts, and guidance of areas that still need attention. Results could be useful in describing what may be occurring in other mines from the region, that have similar characteristics as those studied in these project.

There are still efforts to be made in improving models to monitor these environments, but in general the information retrieved presents a valuable contribution especially to mine managers who usually do not have access to this type of remote sensing tools. The integration of managers in the development of these model could be of great benefit. They could contribute with their field experience and at the same time they can understand the landscape dynamics over time and learn about challenges and limitations when applying remote sensing to monitor mining environments. . This way, models could be tailored to fulfill the expectations and needs of managers in a more efficient way.

.

References

Bachmann, M., Müller, A., Habermeyer, M., Dech, S., 2004. An Iterative Unmixing Approach in Support of Fractional Cover Estimation in Semi-Arid Environments. Proc. of SPIE Remote Sensing Europe, 13-16 September, Masplomas.

Bedini, E., van der Meer, F. and van Ruitenbeek, F. 2009. Use of HyMap imaging spectrometer data to map mineralogy in the Rodalquilar caldera, southeast Spain. International Journal of Remote Sensing, 30:2, pp. 327-348

Ben-Dor, E., Irons, J. R., Epama, G.F., 1999, Soil Reflectance. In: Remote sensing for the earth sciences; manual of remote sensing, 3rd ed., vol. 3, edited by Rencz, A.N., Wiley & Sons, New York, 111-188

Clark, R.N. and Roush, T.L. 1984. Reflectance Spectroscopy: Quantitative Analysis Techniques for Remote Sensing Applications. Journal of Geophysical Research, 89: 6329-6340.

Clark, R.N., King, T.V.V., Klejwa, M., Swayze, G.A. and Vergo, N. 1990. High spectral resolution reflectance spectroscopy of minerals. Journal of Geophysical Research, 95(B8): 12653-12680

Clark, R. N.; Swayze, G. A.; Gallagher, A. J. and King, T. V. V. 1993. Digital spectral library. Version 1: 0.2 to 3.0 microns. U.S. Geological Survey open file report: 93-592.

Clark, R.N., 1999. Chapter 1: Spectroscopy of Rocks and Minerals, and Principles of Spectroscopy. In: A.N. Rencez (Editor), Manual of Remote Sensing, Volume 3, Remote Sensing for the Earth Sciences. John Wiley and Sons, New York, pp. 3-58

Clark, R.N., Swayze, G.A., Wise, R., Livo, E., Hoefen, T., Kokaly, R., Sutley, S.J., 2007, USGS digital spectral library splib06a: U.S. Geological Survey, Digital Data Series 231, http://speclab.cr.usgs.gov/spectral.lib06.

Cowan, W. R. and Robertson, J. G. A. (1999): Mine rehabilitation in Ontario, Canada: tenyears of progress. Proceedings of the Sudbury '99 conference on Mining and the Environment II, Sudbury, ON, Canada, 3: 1037-1043.

Crowley, J.K. et al., 2003. Spectral reflectance properties (0.4-2.5 !m) of secondary Fe- oxide, Fe-hydroxide, and Fe-sulphate-hydrate minerals associated with sulphide-bearing mine wastes. Geochemistry: Exploration, Environment, Analysis, 3(3): 219-228.

Dennison P.; Halligan K. and A. Roberts. 2004. A comparison of error metrics and constraints for multiple endmember spectral mixture analysis and spectral angle mapper. Remote Sensing of Environment 93: 359–367

EGMASA. 2009. Proyecto de Restauracion ambiental del complejo minero de Sotiel Coronada (Calanas, Huelva). Empresa de Gestion Ambiental S. A. Reporte interno.

EPA. 2000. Abandoned Mine Site Characterization and Cleanup Handbook. EPA Regions 8
and 9. EPA 910-B-00-001. August 2000. Available at: www.brownfieldstsc.org/miningsites.cfm.

Ferrier, G., 1999. Application of imaging spectrometer data in identifying environmental pollution caused by mining at Rodarquilar, Spain. Remote Sensing of Environment, 68: 125-137.

Goetz, A.F.H., Vane, G., Solomon, J.E., Rock, B.N. 1985. Imaging Spectrometry for Earth Remote Sensing. Science,228(4704):1147-1153

Gonzalez Romero, Jorge. 2009. Personal comunication. EGMASA, Junta de Andalucia.

Grove C., Hook S., Paylor II E., 1992. Laboratory Reflectance Spectra of 160 Minerals, 0.4 to 2.5 Micrometers. Jet Propulsion Laboratory 92:2.

Hunt, G. R. and Salisbury, J. W. (1970): Visible and near-infrared spectra of minerals and rocks: I. Silicate minerals. Modern Geology 1 (4): 283-300.

Hunt, G. R.; Salisbury, J. W. and Lenhoff, C. J. (1971): Visible and near-infrared spectra of minerals and rocks: III. Oxides and hydroxides. Modern Geology 2 (3): 195-205.

IGME.2004. Manual de restauracion de terrenos y evaluacion de impactos ambientales en mineria. Serie:Guias y manuals 2. Instituto Geologico y Minero de Espana.

Junta de Andalucia. 2006. Evolucion historica de la minera en Andalucia. Junta de Andalucia. Consejeria del ambiente.

Kennedy, .;. Townsend, P.; Gross, E.; Cohen, W.; Bolstad, P.; Wang Y.Q.; and Phyllis Adams. 2009. Remote sensing change detection tools for natural resource managers: Understanding concepts and tradeoffs in the design of landscape monitoring projects. Remote Sensing of Environment 113(7): 1382-1396.

Kemper, T., Haro, J.G., Preissler, H., Mehl, W. and Sommer, S., 2000. A Multiple Endmember Unmixing Approach for Mapping Heavy Metal Contamination After the Donana Mining Accident (Sevilla, Spain), 2nd EARSeL Workshop on Imagning Spectroscopy, 2002.

Kemper, T. 2003. Reflectance spectroscopy for mapping and monitoring of metal

mining related contamination. A case study of the Aznalcollar mining accident, Spain. PhD. Dissertation Thesis, Universität Trier, Germany.

Kemper, T., Sommer S., and J. Garcia. 2005. Assessment of residual soil contamination after the Aznalcollar mining accident (Spain) using multitemporal imaging spectroscopy and spectral mixture analysis. In: Integrated Asessment and management of the ecosystems affected by the Aznalcollar minning spill (SW, Spain), edited by Valls, A. and J. Blasco. UNESCO. p.105-114.

Kleinmann, R.L.P., Crerar, D.A. and Pacelli, R.R., 1981. Biogeochemistry of acid mine drainage and a method to control acid formation. Mining Engineering, 33(3): 300- 305.

Lapakko, K., 2002. Metal Mine Rock and Waste Characterization Tools: An Overview, International Institute for Environment and Development.

Lillesand, T.M., KieferR.W. 1994. Remote sensing and image interpretation. 3rd edition. Wiley & Sons, New York.

Lau, I.C., Hewson, R.D., Ong, C.H, and D. J. Tongway. 2008. Remote mine site rehabilitation monitoring using airborne hyperspectral imaging and landscape function analysis (LFA). The International Archives of the Photogrammetry, Remote Sensing and Spatial Information Sciences Vol. XXXVII. Part B7. Beijing 2008.

Levesque, J . and K. Staenz. 2004. A method for monitoring mine tailings revegetation using hyperspectral remote sensing. Proceedings of Geoscience and Remote Sensing Symposium, 2004, 1 pp. 20-24

Müller, R., Holzwarth, S., Habermeyer, M., Müller, A., 2005. Ortho Image Production within an Automatic Processing Chain for hyperspectral Airborne Scanner ARES, EARSeL Workshop 3D-Remote Sensing, 3D RS Workshop, Porto Portugal.

Olis, M., Nieto, J.M., Sarmiento, A.M., Cer?n, J.C. and C?novas, C.R., 2004. Seasonal water quality variations in a river affected by acid mine drainage: the Odiel River (South West Spain). Science of The Total Environment, 333(1-3): 267-281.

Ong, C. and Cudahy, T.J., 2002. Deriving quantitative monitoring data related to acid drainage using multi-temporal hyperspectral data, 2nd EARSEL Workshop on Imaging Spectroscopy. EARSEL.

Ong, C., Cudahy, T.J. and Swayze, G., 2003a. Predicting Acid Drainage Related Physicochemical Measurements Using Hyperspectral Data, 3rd EARSeL Workshop on Imaging Spectroscopy, 13-16 May 2003, Herrsching, pp. 363-373.

Ong, C., G. Swayze, and R. Clark, 2003b, An investigation of the use of the Tetracorder expert system for multi-temporal mapping of acid drainage-related minerals using airborne hyperspectral data: Proceedings of the 3rd EARSel Workshop onImaging Spectroscopy, May 13-16, 2003, Herrsching, Germany, p. 357-362.

Preissler, H., 1999. Spectral Data Catalogue of the field campaign in the area of the Aznalcollar Mine, Spain (27.05-10.06.99). JRC-SAI/EGEO.

Riaza, A., Ong, C., Müller A., 2006. Dehydration and oxidation of pyrite mud and potential acid mine drainage using hyperspectral DAIS 7915 Data (Aznalcollar, Spain). The international Archives of the Photogrammetry, Remote Sensing and Spatial Information Sciences, Vol. 34, Part XXX.

Richter, N. 2004. Delineation of the Kam Kotia mine tailings areas (Ontario, Canada) using hyperspectral TRWIS III data. M.Sc. Thesis, Universität Postdam, Germany.

Richter, N., Staenz, K. and Kaufmann, H. (2008) 'Spectral unmixing of airborne hyperspectral data for baseline mapping of mine tailings areas', International Journal of Remote Sensing, 29:13, 3937 ? 3956

Richter, R., and Schlaepfer, D., 2002. Geo-atmospheric processing of airborne imaging spectrometry data. Part 2: atmospheric/topographic correction. *Int. J. Remote Sensing* 23:2631-2649

Salomons, W., 1995. Environmental impact of metals derived from mining activities: Processes, predictions, prevention. Journal of Geochemical Exploration, 52(1-2): 5-23.

Santos, A., Prada, J.M. and Rosales, F., 1993. Aspectos geologicos y geofisicos del yacimiento de Migollas. Symposium on the polymetallic sulphides of the Iberian Pyrite Belt, Evora. Apimineral, 1: 8-20.

Sares, M.A. et al., 2004. Characterizing Sources of Acid Rock Drainage and Resulting Water Quality Impacts Using Hyperspectral Remote Sensing - Examples from the Upper Arkansas River Basin, Colorado, 2004 Advanced Integration of GeospatialTechnologies in Mining and Reclamation, Dec. 7-9, 2004, Atlanta, GA.

Singer, P. C. and Stumm, W. (1970): Acidic mine drainage: the rate-determining step. Science 167: 1121-1123.

Specmin-FE, 2003. Spectral Reference Database: Iron Oxides, Selected Iron Sulfates, Iron Oxyhydroxides. Spectral Internation Inc.

Swayze, G.A., Smith, K.S., Clark, R.N., Sutley, S.J., Pearson, R.M., Vance, J.S.,

Hageman, P.L., Briggs, P.H., Meier, A.L., Singleton, M.J., and Roth, S., 2000, Using imaging spectroscopy to map acidic mine waste, Environmental Science and Technology, 34, p. 47-54.

UNEP. 2000. Mining and sustainable development II, challenges and perspectives. Industry and environment. United Nations Environment Programme Divsion of Technology, Industry and Economics.

Zabcic, N., Ong, C. Müller, A., Rivard, B. 2005. Mapping pH from airborne hyperspectral data at the Sotiel-Migollas mine; Calanas, Spain. Proceedings 4th EARSeL Workshop on Imaging Spectroscopy, 27-29th April 2005, Warsaw (Poland).

Zabcic, N. 2008. Derivation of pH-values based on mineral abundances over pyrite mining areas with airborne by hyperspectral data (Hymap) of Sotiel- Migollas mine complex. M.Sc. Thesis, University of Alberta, Canada, 154 pp.

APPENDIX 1

Mineral composition, according to XRD analysis, of soil samples collected from the ashes dam of the Sotiel Migollas mine during field campaing of 2008

Soil Sample	Mineral compostion XRD analysis
Sample 1 	Starkeyite $MgSO_4 \cdot 4H_2O$ Rozenite $FeSO_4 \cdot 4H_2O$ Ilesite $(Mn,Zn,Fe)SO_4 \cdot 4H_2O$ Boylenite $(Zn,Mg)SO_4 \cdot 4H_2O$ Gypsum Pickeringite
Sample2 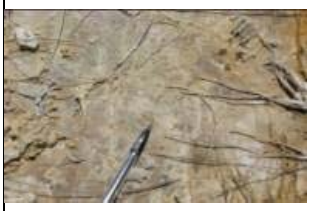	Gypsum (Ca, S) Hydronium jarosite (Fe, S, K) Quartz Clay minerals (muscovite, chlorite, illite) (Si, Al, Mg, Fe, K, Na) Limonite
Sample3 	Gypsum (Ca, S) Hydronium jarosite Quartz (Si) Starkeyite Schwetmannite (Fe, S, K) Clay minerals (muscovite, chlorite, illite) (Si, Al, Mg, Fe, K, Na) Limonite
Sample 4 	Gypsum Hydronium jarosite Quartz Starkeyite Schwertmannite Clay minerals (muscovite, chlorite)
Sample 5 	Gypsum Starkeyite Pickeringite/halotrichite Hexahydrite Kieserite Copiapite Hydronium jarosite.

Sample 12 	Gypsum Starkeyite Quartz Clay minerals (clinochlore)
Sample 13 	Gypsum Quartz Hexahydrite Clay minerals (clinochlore)
Sample 14 	Gypsum Hydronium jarosite Quartz Goethite Rostite(?)
Sample 15 	Gypsum Hydronium jarosite Goethite Quartz
Sample 16 	Gypsum Hydronium jarosite Quartz

APPENDIX 2

Spectra of iron oxide, iron hydroxide, iron sulphate and sulphide minerals related to pyrite oxidation (Crowley et al., 2003).

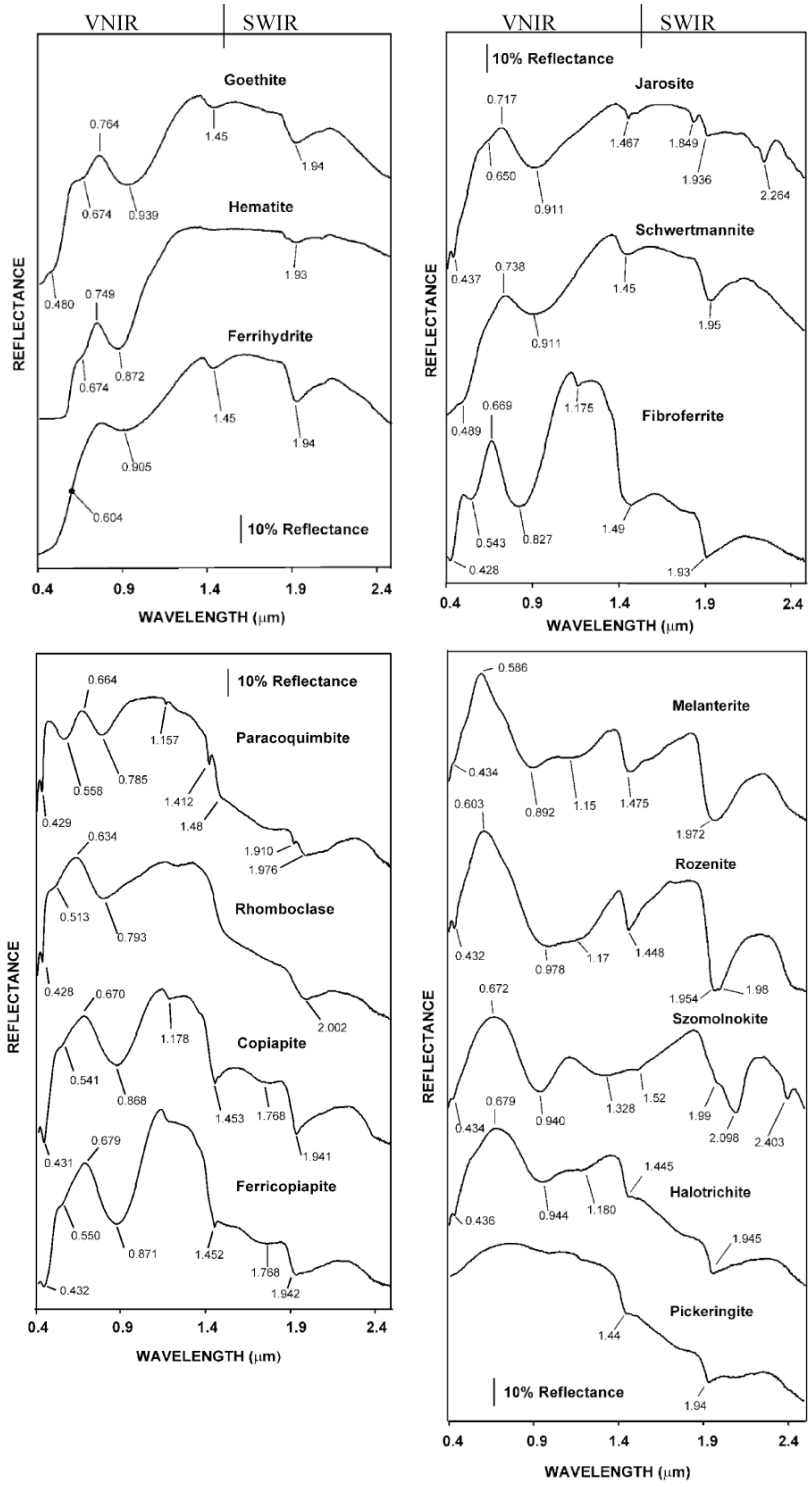

APPENDIX 3

Mineral maps for mining area and tailing area obtained by Richter (2008) in the Sotiel Migollas mine for 2004.

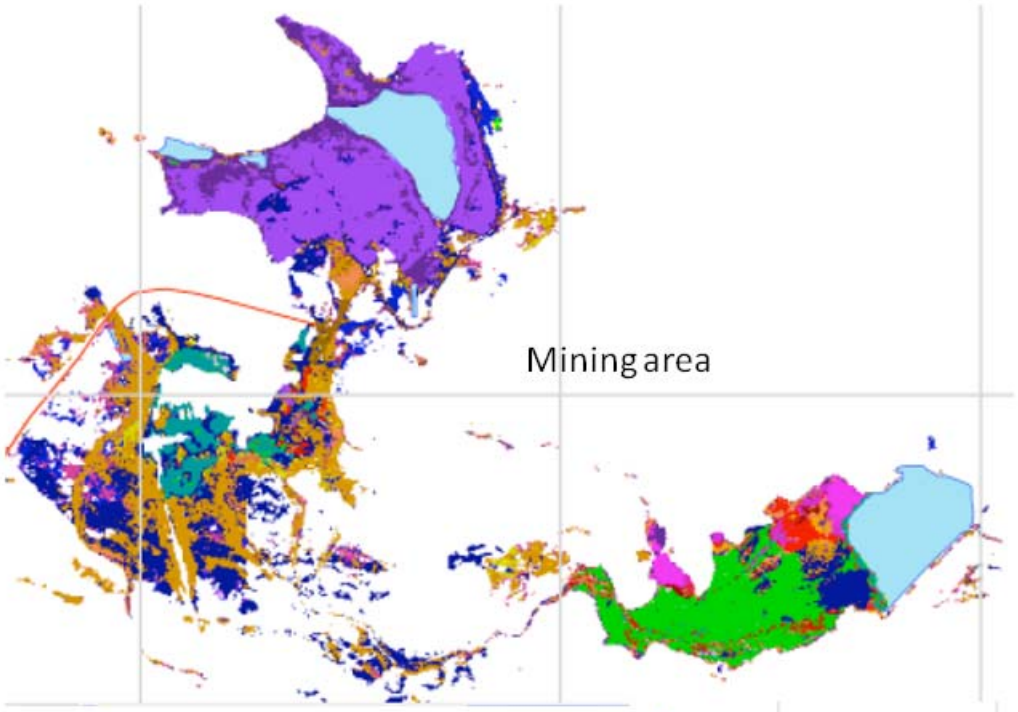

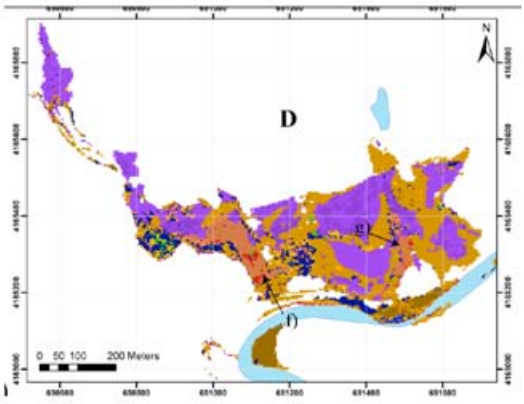

EM 1 - **GT**, mu, al
EM 8 - **GT**, al
EM 2 - **GT**-SCH, mu, al
EM 3 - **GT-JR**, mu, al
EM 5 - SCH-JR, al, mu
EM 7 - **SCH**, gt, cl, qz, mu and/or al
EM 22 - **SCH-JR**, al and/or mu
EM 4 - Soils with SCH/FERR, gt, mu, al
EM 6 - Soils with GT-FERR
EM 23 - **HE**, mu, al
EM 24 - **HE**
EM 25 - **HE**, cl
EM 9 - **JR-GT**, mu, al
EM 21 - **JR**-SCH, ferr, al, mu, qz
EM 10 - **HA**, sch, al, alu, gp
EM 11 - **HA**, rh
EM 12 - HA-jr
EM 14 - **HA**, rz
EM 20 - HA-CO
EM 18 - **CO**, jr, sch
EM 19 - **CO**, me, sch
EM 17 - **PK-HA**-SZ
EM 13 - RZ-HA
EM 15 - RZ
EM 16 - SZ-HA, py
EM 26 - **PY**-SZ

APPENDIX 4

Mineral map of mine waste draped over a digital elevation model (Zabcic 2008)